

Seasonal variations in viral distribution, dynamics and viral mediated host mortality in the Arabian Sea.

Aparna S.¹, Parvathi A.^{1*}, Jasna V.^{1,2}, Pradeep Ram A. S.³ and Sime-Ngando T.³

¹ CSIR-National Institute of Oceanography, Regional Centre (CSIR), Kochi-682 018, India

² Department of Aquatic Life Medicine, College of Fisheries Science,
Pukyong National University, Busan, Republic of Korea

³ Laboratoire Microorganismes : Génome et Environnement, UMR CNRS 6023,
Université Clermont-Auvergne, 1 Impasse Amélie Murat, 63178 Aubière Cedex, France

* Corresponding author: Dr. Parvathi A

CSIR-National Institute of Oceanography Regional Centre, Dr. Salim Ali Road,
Post Box No. 1913, Kochi-682 018, India

Ph: 91-(0) 484-2390814, Fax: 91-(0) 484-2390618

Email: parvathi@nio.org

Running page head: Seasonal variations in viral activities in the Arabian Sea

Abstract

Viruses are key players in the marine ecosystem. It is critical to study specific viral processes and their interrelationship with various biotic and abiotic variables to quantify their impact on the marine environment. This study investigates the influence of seasonality on viral distribution and their mediated processes in the coastal region of the southeastern Arabian Sea (India) for two consecutive years (2014 and 2015). Water samples were collected from four sampling stations, S1, S2, S3 and S4, in the southeastern Arabian Sea on a monthly basis. Samples were analyzed for the variations in viral abundance, viral production, and viral-induced host mortality covering three seasons namely, pre-monsoon, monsoon and post-monsoon. Viruses and bacteria were enumerated by epifluorescence microscopy following staining with SYBR Green I and viral production was estimated using viral dilution method. Seasonal variations in viral mediated mortality and microzooplankton grazing mortality of phytoplankton hosts were estimated by modified dilution method. The results revealed a pronounced seasonal pattern of viral abundance ($0.04-4.03 \times 10^7$ viruses mL⁻¹) and viral production ($0.71 \times 10^{10}-4.94 \times 10^{10}$ L⁻¹d⁻¹). The observed high viral-induced mortality of prokaryotes (25.85%) and phytoplankton (7.98–28.9%) during the pre-monsoon season was eventually linked to high viral abundance and production rates. Viral mediated processes were essentially linked to host density and water temperature. Transmission electron microscopy analysis revealed that myoviruses and non-tailed viruses were dominant in the study region with rod shaped bacteria being more susceptible to viral infection. The results indicated the prevalence of seasonally induced active viral processes in this tropical marine ecosystem which may significantly contribute to rapid recycling of nutrients in this region.

Keywords: Marine virus, viral induced prokaryotic mortality, viral production, viral morphotypes, nutrient recycling

Introduction

Viruses are the most numerous (10^{10} viruses per litre of seawater) and smallest biological entities in the marine environment which are capable of infecting almost all organisms. Viral mediated host lysis impacts marine biogeochemical cycles, host community composition, diversity and host evolution (Breitbart et al. 2018). Prokaryotes are the major hosts for marine viruses and phage numbers are highly correlated to prokaryote counts (Wommack and Colwell 2000; Jasna et al. 2017; Parvathi et al. 2018). Viral abundance is highly variable with respect to space and time. Short term to long term dynamics of viral abundance have been reported from different geographic locations (Rodriguez et al. 2000; Taylor et al. 2003; Clokie et al. 2006; Thomas et al. 2010; Parvathi et al. 2015; Jasna et al. 2017). Generally, viral abundance is highest in the euphotic zone and coastal environments compared to deeper waters and oligotrophic environments (Wommack and Colwell 2000; Parsons et al. 2012; Parvathi et al. 2018). However, subsurface peaks of viral abundance were observed in the mid latitude regions of the North Pacific (Yang et al. 2010). Studies also show that viral abundance and distribution are greatly influenced by the abundance and activities of their abundant hosts such as prokaryotes and phytoplankton (Taylor et al. 2003; Parsons et al. 2012; Gainer et al. 2017). Apart from prokaryotic abundance and chlorophyll *a* concentration, environmental variables like nutrients, temperature, salinity, sunlight, etc. are significant predictors of viral abundance in varying marine environments (Finke et al. 2017). Viral mediated mortality is also largely variable and have differential impacts on bacterial production in systems with different trophic status. Compared to grazer mediated mortality, viral mediated host mortality at times can dominate depending on the environment (Bettarel et al. 2004). Investigation across the North Atlantic Ocean reported viral mediated mortality as the major phytoplankton loss factor in the low and mid latitudes. Whereas, grazer mediated mortality dominated at higher latitudes (Mojica et al. 2016). Various studies have highlighted the importance of viral-mediated nutrient cycling over direct effect of viral-induced mortality, for promoting the growth of non-infected phytoplankton and bacterial populations (Weinbauer et al. 2011; Shelford et al. 2012).

The Arabian Sea has a unique hydrography influenced mainly by the seasonal reversal of monsoonal winds with high biological productivity. High primary productivity and existence of intense oxygen minimum zones (OMZ) and denitrification zones make the Arabian Sea a unique oceanic region (Naqvi et al. 1990; Olson et al. 1993; Gerson et al. 2014). During spring inter monsoon, the water column remains warmer and highly stratified with nutrient deficient surface waters, whereas, wind driven coastal upwelling during southwest monsoon and convective overturning of surface waters due to winter cooling in the northeast monsoon render the water column well mixed during both the monsoons (Prasanna Kumar and Prasad 1996; Gerson et al. 2014). Several studies have reported

seasonal variations in bacterial abundance and primary productivity associated with physical forcing in the Arabian Sea (Campbell et al. 1998; Ramaiah et al. 2009). High primary productivity during the southwest monsoon was found to be associated with high nutrient availability (Prasanna Kumar et al. 2000). The physical forcing in the Arabian Sea arising from a unique combination of climate, wind, and circulation imparts seasonal variations in trophic conditions and brings in huge diversity (Burkhill et al. 1993; Mantoura et al. 1993). Some of the investigations conducted in the Arabian Sea concluded a close coupling of bacterial production with primary production during summer and winter monsoons (Wiebinga et al. 1997). During high primary production, the labile (rapidly degradable) dissolved organic carbon (DOC) produced by phytoplankton are rapidly used by the bacteria (in hours or days). In contrast, at time of low primary production, high bacterial abundance and production may be sustained by semi-labile DOC that can last from weeks to months in the water column (Calleja et al. 2019). Thus, at both times (during high and low primary production) the DOC pool is sustaining bacterial growth. High bacterial abundance and production at time of low primary production, especially during the spring and fall inter monsoons suggests of predominance of microbial loop in the sustenance of the dissolved organic carbon (DOC) pool (Ducklow 1993; Ramaiah et al. 1996; Campbell et al. 1998). A recent report by Sabbagh et al. (2020) suggests that heterotrophic bacteria are controlled by viruses most of the year in the coastal waters of the Red sea. This indicates that viral-induced mortality is one of the major regulators that control bacterioplankton standing stocks.

To date, few reports are available on viruses in the Arabian Sea (Brum et al. 2013; Jain et al. 2014; Parvathi et al. 2018). Parvathi et al. (2018) have studied the viral abundance, viral processes and viral life strategies in the oxygen minimum zones of the Arabian Sea. The morphological diversity of the viruses and their characteristic features were examined as a part of TARA Ocean expedition (Brum et al. 2013). Jain et al. (2014) reports on the seasonal variations in viral abundance and virus-to prokaryote ratio. However, no information exists on the seasonal variations in viral processes in the Arabian Sea to date. To better understand the impact of viruses in the marine environment, it is critical to study specific viral processes and their interrelationship with various biotic and abiotic variables. Moreover, estimation of parameters like viral production, turnover rates, and viral mediated mortality are essential for the incorporation of viral processes into various ecosystem models. Recent studies by Jasna et al. (2017, 2019) from an estuarine region (Cochin estuary) in the southwest coast of India reports on the seasonal variations in viral abundance, viral production and viral process. These studies reveal that distinct seasons such as monsoon, pre- and post-monsoons have profound influence on viral abundance and production. The present study is one among the few in the Arabian Sea, specifically the southeastern Arabian Sea, to investigate the seasonality in viral distribution and viral processes.

We hypothesize that there could be a significant seasonal variation in the viral distribution and viral mediated mortality in the study region and viral lysis may play a significant role in the microbial loop in this part of the southeastern Arabian Sea.

Materials and methods

Sampling locations, physical and chemical parameters

Water samples were collected from four sampling stations, S1, S2, S3 and S4, located in a transect perpendicular to the coast of Kochi (south west coast of India), in the eastern Arabian Sea (Fig 1). Station S1, has a depth of ~30 m whereas, S2, S3, and S5 have a depth of 22 m, 14 m and 6 m, respectively. Samples were collected during three distinct seasons namely, pre-monsoon (PRM), monsoon (M) and post-monsoon (PM) from three depths (surface, middle and bottom) of S1 (0.5 m, 15 m and 30 m), S2 (0.5 m, 11 m, and 22 m), and S3 (0.5 m, 7 m, and 14 m), and from two depths of S4 (0.5 m and 6 m) on a monthly basis for two consecutive years, 2014 and 2015. Totally 253 samples were collected from all the four stations in the study. In June 2014 (M), sampling was not done due to adverse climatic conditions. Water samples were collected using a 5L Niskin sampler (Hydro-Bios, Germany). Samples were transferred to acid washed sterile glass bottles and were transported to the laboratory in an ice box maintained at 4°C. Vertical profiles of temperature and salinity were recorded using a conductivity temperature density (CTD) profiler (SBE Seabird 19, Sea-Bird Scientific, Bellevue, WA, USA) with accuracy $\pm 0.001^\circ\text{C}$ and ± 0.001 S/m for temperature and conductivity, respectively. Samples for dissolved oxygen (DO) were withdrawn from the niskin sampler into DO bottles (60 mL) without trapping air bubbles, allowing the bottles to overflow with at least one liter to avoid exchange with atmospheric oxygen. The dissolved oxygen in the bottle was fixed with 0.5 mL each of Winkler reagents and estimated by Winkler's titration method (Grasshoff 1983). Inorganic nutrients such as nitrate, nitrite and phosphate present in the water samples were estimated by spectrophotometric analysis (Grasshoff 1983). To determine the Chl *a*, samples were first filtered through 0.7 μm GF/F (Whatman, USA), treated with 90% acetone overnight in dark at 4°C, and the pigment was measured fluorometrically (Parsons et al. 1984).

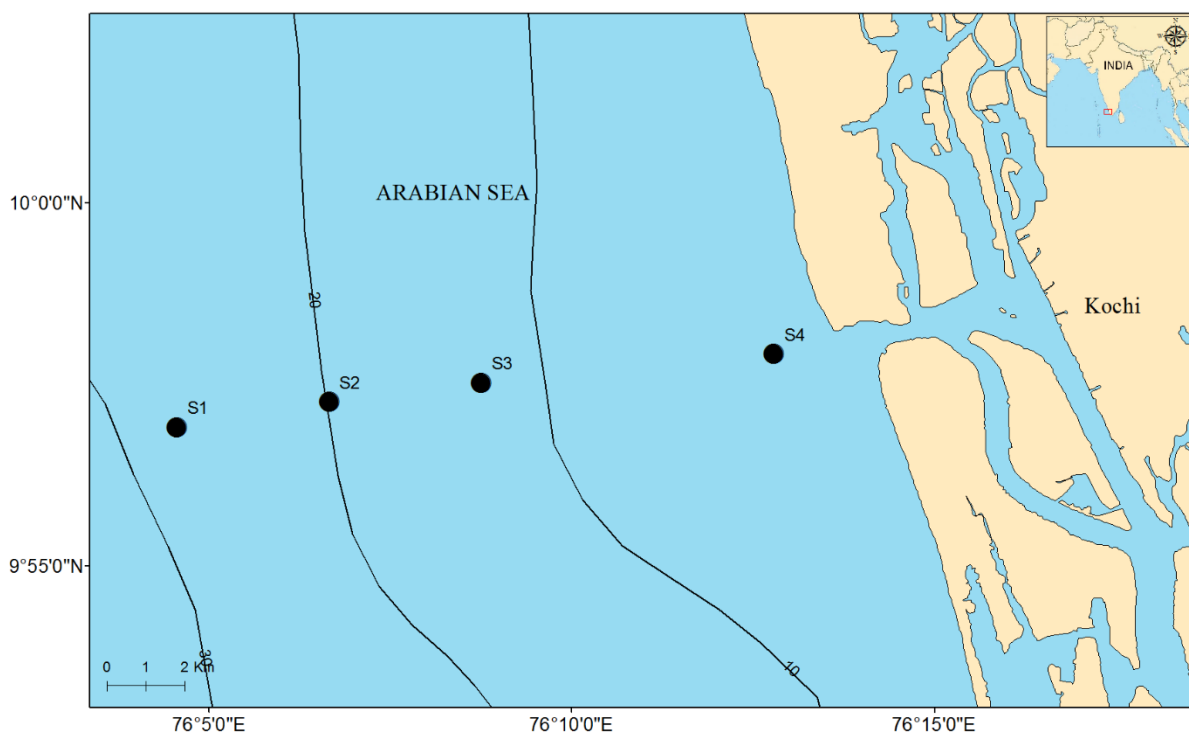


Fig. 1 Sampling locations in the Arabian Sea. Water samples were collected from four stations of a transect perpendicular to the coast of Kochi on monthly basis during 2014 and 2015. Sampling locations are marked as S1, S2, S3 and S4

Abundance of viruses and prokaryotes

Viruses and bacteria in the sample were enumerated by epifluorescence microscopy following the SYBR Green I staining method (Patel et al. 2007). Immediately after collection, 1 mL each of the samples were fixed with formalin (37% (w/v) formaldehyde, 0.02 μm filtered) to a final concentration of 2% (v/v). The samples were then kept on ice for 10 min in dark and subsequently filtered (< 20 KPa vacuum) through 0.02 μm Anodisc filters (Whatman). The filters were dried completely and stained with 100 μL each of 1:40 diluted SYBR Green I commercial stock for 20 min. Excess stain was removed and the filters were mounted on glass slides with 30 μL of 0.1% (v/v) anti-fade mounting medium (*p*-phenylenediamine). The slides were observed under an epifluorescence microscope (Olympus BX 41, Olympus, USA) for the enumeration of viruses and prokaryotes. Prokaryotes and viruses could be distinguished from each other based on their relative sizes. Viruses appeared as numerous green pinpricks, whereas, bacteria were larger and possessed definite shapes. A blank was routinely examined as a control for contamination of equipment and reagents.

Viral Production and turnover rates

Viral production rates in the surface water samples of stations S1 and S4 during the three seasons (pre monsoon, PRM; monsoon, M; post monsoon, PM) in the year 2014 were estimated by diluting the water sample (100 mL) in triplicates with three volumes of ultra-filtered (using CDUF001LT, Millipore, USA, with a membrane having molecular weight cut-off or MWCO of 100 kDa) virus-free seawater and subsequently incubating them at room temperature (30°C) in the dark for 24 h. Subsamples (1 mL) were collected every 3 h to enumerate viruses and prokaryotes (Wilhelm et al. 2002). Viral production rates were estimated from the first order regression of increase in viral abundance over time, after correcting for the dilution of prokaryotes in the experimental sample, using the formula, Viral production, $VP = m \times (P/p)$, where 'm' is the slope of the regression line, 'p' is the concentration of prokaryotes after dilution, and 'P' is the concentration of prokaryotes prior to dilution. Viral turnover rates (VTR) were estimated from the ratio of viral production to viral abundance in the undiluted sample.

Viral induced prokaryotic mortality (VIPM) and phenotypic diversity of viruses

In order to determine the prokaryotic mortality due to viral lysis, surface water samples from S1 and S4 during the three seasons (PRM, M and PM) were collected and fixed with formalin (final concentration of 2% v/v). Prokaryotic cells in the sample were gathered on a 400-mesh formvar grid by ultracentrifugation (Beckman Coulter SW40 Ti Swing-Out-Rotor, 70,000 × g, 20 min at 4°C). The grids were stained with uranyl acetate (2% w/w) for 30 s and washed twice with 0.02-μm filtered distilled water and dried completely (Pradeep Ram et al. 2010). The stained grids were observed using a JEOL 1200EX transmission electron microscope (20,000-60,000 X magnification). Frequency of visibly infected cells (FVIC) were determined by examining 600-800 prokaryotic cells per grid. A minimum of 15 infected cells were examined to determine the average burst size (BS). Frequency of infected cells (FIC) and viral induced prokaryotic mortality (VIPM) were estimated using the following formulae: $FIC = 9.524 FVIC - 3.256$ (Weinbauer et al. 2002) and $VIPM = (FIC + 0.6 \times FIC^2)/(1 - 1.2 \times FIC)$ (Binder 1999). During the transmission electron microscopy analysis, visualization of viruses was performed at a magnification of 65,000-1,00,000. Viruses were classified as myoviruses, podoviruses, siphoviruses, and non-tailed viruses based on their morphology (Borrel et al. 2012)

Viral mediated mortality (VMM) and microzooplankton grazing mortality (MGM) of phytoplankton hosts

Seasonal variations in viral mediated mortality (VMM) and microzooplankton grazing mortality (MGM) of phytoplankton hosts in the surface waters of S1 and S4 were estimated by modified dilution method (Evans et al. 2003). Samples were collected during the three seasons: PRM, M and PM. Two parallel dilution series (20%, 40%, 70% and 100%) of the whole seawater, one with grazer-free diluent (0.2- μm filtered) and the other with virus-free diluent (100 kDa filtered), were prepared after removing the mesoplankton size fraction through a 200 μm nylon mesh (1L final volume). The bottles were incubated under *in situ* conditions of temperature (28-30 °C) and light for a period of 24 h. Subsamples were collected at 0 h and 24 h for the enumeration of phytoplankton host populations. Apparent growth rate (k , d^{-1}) of phytoplankton in each bottle were calculated using the equation,

$$k = \ln(P_t/P_0)/t$$

where ‘ P_0 ’ and ‘ P_t ’, respectively, are the plankton abundance before and after incubation and ‘ t ’ is the time interval for the incubation.

A first order regression of apparent growth rate against fraction of seawater (for both 0.2 μm and 100 kDa) was used for the estimation of mortality due to grazing (m_g) and combined mortality due to grazing and viral lysis (m_{g+v}) for those incubations that produced significantly different regression slopes for the two dilution series as determined from an F-test. Regression coefficients of the 0.2 μm series and the 100 kDa series represent the microzooplankton grazing rates (m_g) and the combined mortality rates of microzooplankton grazing and viral lysis (m_{g+v}), respectively (Evans et al. 2003; Ortmann et al. 2011; Cram et al. 2016). Viral mediated mortality (m_v) can be estimated using the formula,

$$m_v = m_{g+v} - m_g$$

Percentage of viral mediated mortality and microzooplankton grazing mortality were estimated using the equations,

$$\% VMM = (1 - e^{-m_v}) \times 100$$

$$\% MGM = (1 - e^{-m_g}) \times 100$$

Statistical analysis

Potential relationship among different biological, physical and chemical variables were tested by Pearson correlation analysis. Principal component analysis (PCA) using PAST software version 3

(Hammer et al. 2001) was also employed for analyzing the major variables influencing viral abundance and dynamics during the three distinct seasons. To discern the biotic and abiotic predictor variables which drive the seasonal variations in viral abundance, a distance based linear modeling analysis (distLM) was performed using Primer 7 software (McArdle and Anderson 2001). Significant inter-annual, seasonal and spatial variability in different biotic and abiotic variables were tested by three-way ANOVA using the trial version of SPSS software.

Results

Spatial and vertical variability in physical and chemical parameters

Temperature varied vertically along the water column. Surface waters had an average temperature of $29.25 \pm 1.34^\circ\text{C}$ in 2014 and $29.25 \pm 1.87^\circ\text{C}$ in 2015 (Average values of all stations combined). Middle and bottom waters were cooler than surface waters. In all the three seasons, highest temperature was recorded in the surface waters at all the four stations (Online Resource 3). DO exhibited significant spatial variability ($p < 0.001$) and varied between depths in all the stations with the surface having the highest value compared to middle and bottom (Tables 2 & 3). The lowest values of DO were estimated from the bottom waters of all the stations during M except for station 4 in 2014 which had the highest DO concentration in bottom waters during monsoon (7.11 mL L^{-1}). Salinity of the four stations varied significantly ($p < 0.001$) with the offshore stations (S1 and S2) having higher salinities when compared to near-shore stations (S3 and S4). The average salinity at S1 was recorded as 34 ± 2.45 in 2014 and 34.02 ± 1.26 in 2015. Whereas, at S4, the salinity was 30.8 ± 0.74 and 32.7 ± 2.4 in the years 2014 and 2015, respectively. The salinity of near-shore stations was influenced by the freshwater input from the Cochin estuary with maximum influx during south west monsoon and least during PRM periods. The seasonal values of salinity varied significantly ($p < 0.05$) between the two years. Chl *a* also exhibited significant spatial variations ($p < 0.001$) with highest concentrations at the near-shore stations as compared to offshore stations (Tables 2& 3). Concentrations of dissolved inorganic nutrients like NO_3 and PO_4 were higher in bottom waters as compared to surface waters (Tables 2& 3). NO_3 concentration of the water column ranged from $0.05\text{-}24.47 \mu\text{mol L}^{-1}$ in 2014 and $0.1\text{-}22.41 \mu\text{mol L}^{-1}$ in 2015. Nitrogen to Phosphorous (NP) ratio of the study region ranged from $0.33\text{-}18.21$ in 2014 and $0.52\text{-}19.67$ in 2015.

Seasonal variability in physical and chemical parameters

Each year was divided into three seasons, PRM, M and PM for comparison. Seasonal variations were prominent for most of the parameters studied. In both the years, temperature was maximum during PRM ($29.81 \pm 0.8^\circ\text{C}$ in 2014 and $30.14 \pm 0.72^\circ\text{C}$ in 2015), followed by PM ($28.93 \pm 0.6^\circ\text{C}$ in 2014

and $28.67 \pm 0.44^\circ\text{C}$ in 2015) and the lowest during M ($26.41 \pm 1.59^\circ\text{C}$ in 2014 and $24.98 \pm 1.13^\circ\text{C}$ in 2015) (Online Resource 1). Salinity was highest during PRM and averaged 33.95 ± 1.09 in 2014 and 33.62 ± 1.96 in 2015 (Online Resource 1). The lowest salinity was observed during M with average values of 30.23 ± 1.76 in 2014 and 29.98 ± 2.11 in 2015. However, the seasonal variations in salinity was not significant statistically. Dissolved oxygen (DO) concentrations exhibited significant seasonal variability ($p < 0.001$) (Table 1). The PM season had the highest DO concentrations ($6.19 \pm 1.87 \text{ mL L}^{-1}$ in 2014 and $7.89 \pm 1.54 \text{ mL L}^{-1}$ in 2015), whereas, PRM was estimated to have the lowest DO in both the years ($4.82 \pm 1.48 \text{ mL L}^{-1}$ in 2014 and $4.83 \pm 2.97 \text{ mL L}^{-1}$ in 2015). Concentrations of nutrients like NO_3 , SiO_4 and PO_4 had significant seasonal variations ($p < 0.001$) with highest values during M and the least during PRM. NO_3 concentration in the water column ranged $0.45\text{-}24.47 \mu\text{mol L}^{-1}$ (in 2014) and $0.17\text{-}22.41 \mu\text{mol L}^{-1}$ (in 2015) during M and $0.05\text{-}2.42 \mu\text{mol L}^{-1}$ (in 2014) and $0.30\text{-}3.97 \mu\text{mol L}^{-1}$ (in 2015) during PRM. Chl *a* concentration was significantly high during M ($4.45 \pm 0.8 \text{ mg m}^{-3}$) and low during the other two seasons ($0.68 \pm 0.74 \text{ mg m}^{-3}$ and $0.61 \pm 0.50 \text{ mg m}^{-3}$ during PRM and PM, respectively) (Online Resource 1). The Chl *a* concentration increased by 2 to 5-fold from PRM to M (Online Resource 1). At the nearshore stations, Chl *a* was comparatively high during all the seasons indicating the influence of nutrient input from the estuary.

Inter-annual variability in physical and chemical parameters

The average values (calculated for each depth of the four stations) of physical, chemical and biological variables in the three seasons of the two years are listed in Tables 2 and 3. Dissolved oxygen, NH_4 , SiO_4 and PO_4 showed significant inter-annual variations ($p < 0.001$) (Table 1). DO concentrations (of all depths and stations) ranged from $0.21\text{-}11.90 \text{ mL L}^{-1}$ in 2014, and $0.58\text{-}10.92 \text{ mL L}^{-1}$ in 2015 in the study area. The average dissolved inorganic nutrient concentration (of all depths and stations) was highest in 2014 (NH_4 , $5.58 \pm 7.81 \mu\text{mol L}^{-1}$; PO_4 , $0.86 \pm 0.84 \mu\text{mol L}^{-1}$; SiO_4 , $11.76 \pm 8.49 \mu\text{mol L}^{-1}$) as compared to 2015 (NH_4 , $3.20 \pm 2.88 \mu\text{mol L}^{-1}$; PO_4 , $0.40 \pm 0.38 \mu\text{mol L}^{-1}$; SiO_4 , $8.74 \pm 9.05 \mu\text{mol L}^{-1}$). Temperature, salinity and Chl *a* exhibited no significant inter-annual variations. Temperature ranged from $23.05\text{-}31.57^\circ\text{C}$ in 2014 and $23.09\text{-}31.87^\circ\text{C}$ in 2015 (of all depths and stations). Seasonal variation in temperature between the two years was prominent in the study area ($p < 0.05$). The average salinity was 33.08 ± 3.75 in 2014 and 33.56 ± 1.89 in 2015 (Average value of all depths, and stations). Chl *a* concentration in the study region ranged $0.03\text{-}30.60 \text{ mg m}^{-3}$ in 2014 and $0.01\text{-}30.60 \text{ mg m}^{-3}$ in 2015.

Variations in viral and prokaryotic abundance

Seasonal variations in viral and prokaryotic abundances were significant in all the stations with PRM having the highest abundance followed by PM and M (Fig 2). Viral abundance (VA) (represented as viral like particles or VLPs) showed significant ($p < 0.001$) inter-annual variations (Table 1) ranging from $0.07\text{-}2.08 \times 10^7$ VLP mL^{-1} in 2014 and $0.04\text{-}4.03 \times 10^7$ VLPs mL^{-1} in 2015 (values from all depths and stations). Viral and prokaryotic abundances varied significantly among stations ($p < 0.05$ and $p < 0.001$, respectively). The average VA (all depths combined for each station) was significantly greater at the near-shore stations ($0.46 \pm 0.37 \times 10^7$ VLPs mL^{-1} in 2014 and $0.72 \pm 0.8 \times 10^7$ VLPs mL^{-1} in 2015) as compared to the offshore stations ($0.34 \pm 0.22 \times 10^7$ VLPs mL^{-1} in 2014 and $0.74 \pm 0.63 \times 10^7$ VLPs mL^{-1} in 2015). In general, highest abundances were estimated in the surface waters followed by middle and bottom waters (Tables 2 & 3). However, there was no statistically significant variations in VA between these three depths. Prokaryotic abundance (PA) ranged from $0.17\text{-}3.3 \times 10^6$ cells mL^{-1} during 2014 and $0.01\text{-}4.71 \times 10^6$ cells mL^{-1} during 2015. Although there was a similar vertical pattern of PA as that of VA, the variations were not statistically significant. PA also exhibited seasonal and spatial variations (Tables 2 & 3). VA was positively correlated to PA ($p < 0.001$) and Chl *a* ($p < 0.005$), whereas, PA showed significant positive correlations with temperature ($p < 0.001$) and DO ($p < 0.001$).

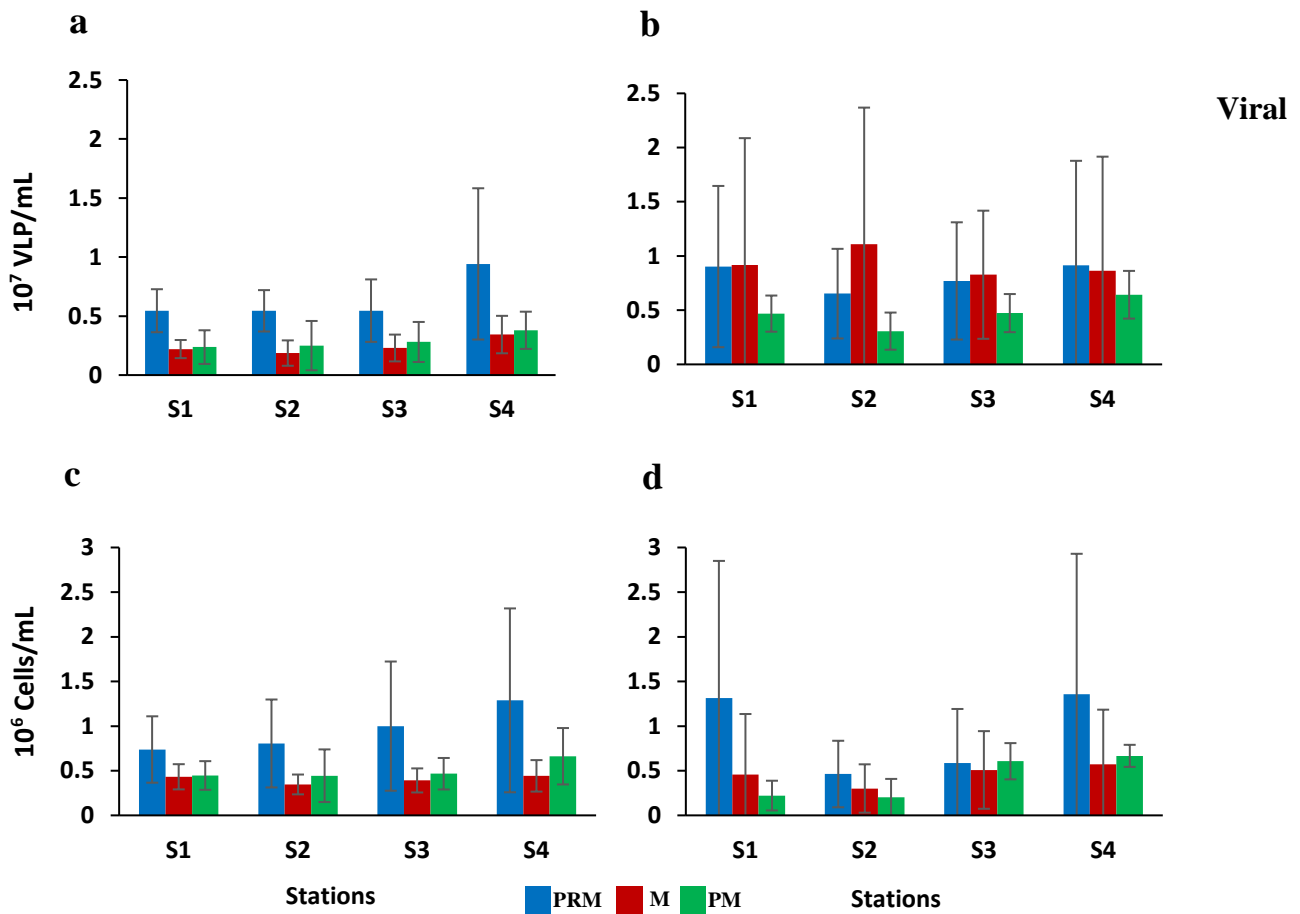


Fig. 2 Variations in viral and prokaryotic abundance (VA & PA) during pre-monsoon (PRM, blue), monsoon (M, red) and post monsoon (PM, green) seasons. (a) VA in 2014, (b) VA in 2015, (c) PA in 2014 and (d) PA in 2015

production (VP) and viral turnover rates (VTR) in surface waters

VP and VTR from surface waters during the three seasons of 2014 are presented in Fig. 3. Viral production rates were higher during PRM ($4.48 \pm 0.83 \times 10^{10} \text{ L}^{-1}\text{d}^{-1}$ at S1 and $4.94 \pm 1.6 \times 10^{10} \text{ L}^{-1}\text{d}^{-1}$ at S4), followed by PM ($1.93 \pm 0.86 \times 10^{10} \text{ L}^{-1}\text{d}^{-1}$ at S1 and $3.16 \pm 0.63 \times 10^{10} \text{ L}^{-1}\text{d}^{-1}$ at S4) and lowest during M ($0.71 \pm 0.63 \times 10^{10} \text{ L}^{-1}\text{d}^{-1}$ at S1 and $1.45 \pm 0.87 \times 10^{10} \text{ L}^{-1}\text{d}^{-1}$ at S4). Viral turnover rates (VTR) ranged from 9.04-46.39 d^{-1} and followed the same pattern as VP except that S1 had the highest turnover rates compared to S4.

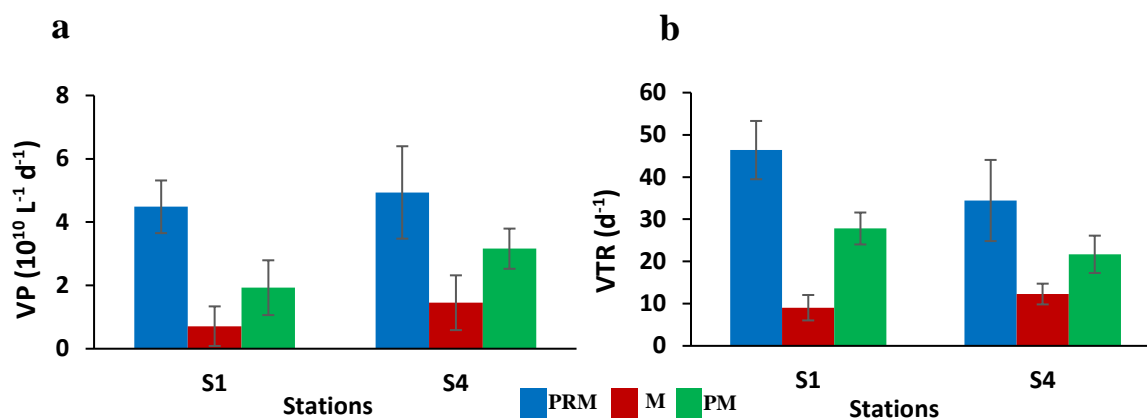


Fig. 3. Variations in (a) viral production (VP) and (b) viral turnover rates (VTR) at stations S1 and S4 during pre-monsoon (PRM, blue), monsoon (M, red) and post monsoon (PM, green) in 2014

induced prokaryotic mortality (VIPM) as determined by TEM analysis

FIC averaged $17.7 \pm 2.33\%$, $7.3 \pm 1.86\%$ and $10.79 \pm 2.87\%$ for PRM, M and PM, respectively (Fig. 4). VIPM, which was estimated from FIC and it ranged from 5.86-28.64% with an average of $13.63 \pm 7.19\%$. The annual average of VIPM at S1 and S4 were $15.16 \pm 6.63\%$ and $12.09 \pm 7.75\%$, respectively. PRM was marked with the highest VIPM ($24.15 \pm 6.35\%$ at S1 and $25.85 \pm 3.95\%$ at S4) compared to other seasons (Fig. 4).

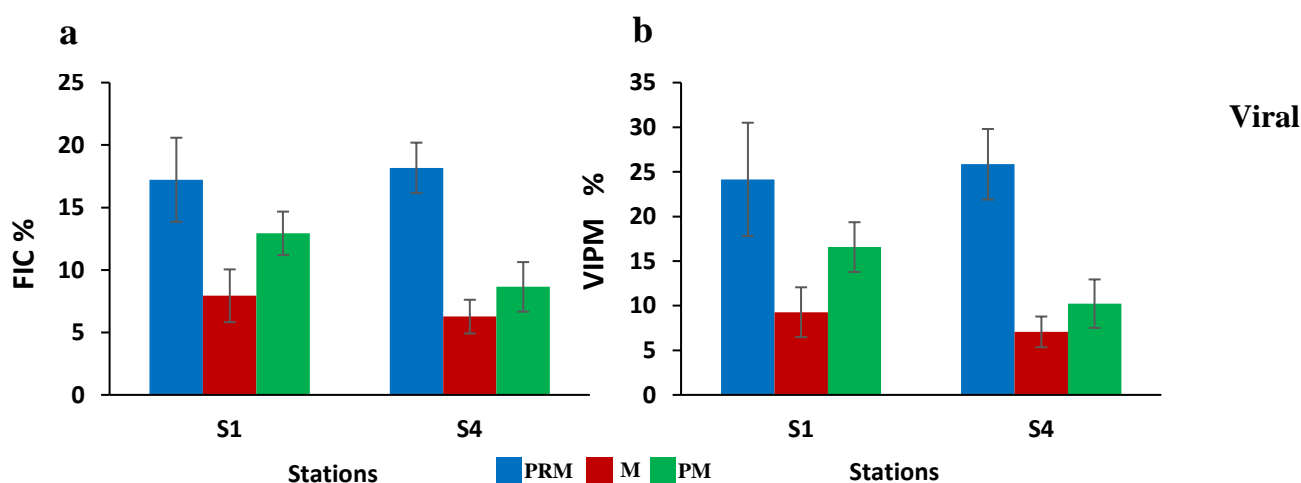


Fig. 4 Seasonal variations in (a) frequency of infected cells (FIC) and (b) viral induced prokaryotic mortality (VIPM) at S1 and S4 in 2014. Pre-monsoon (PRM): blue; monsoon (M): red; post monsoon (PM): green

mediated mortality (VMM) of phytoplankton by the modified dilution method

The modified dilution experiment was carried out to estimate the viral mediated mortality (VMM) and microzooplankton grazing mortality (MGM) of phytoplankton during PRM, M and PM in 2014 for

water samples collected from S1 and S4 (Fig. 5). VMM was greater during PRM ($28.9 \pm 11.35\%$ and 26.24% at S1 and S4, respectively), followed by PM ($7.98 \pm 2.65\%$ and $9.83 \pm 1.36\%$ at S1 and S4, respectively). Lowest mortality was observed during M ($10.78 \pm 12.71\%$ at S1 and $13.7 \pm 6.67\%$ at S4). MGM followed the same pattern at S1 ($14.91 \pm 4.97\%$, $6.47 \pm 0.65\%$ and $10.21 \pm 5.4\%$ during PRM, M and PM, respectively). However, at S4, MGM was greater during PM ($19.12 \pm 3.82\%$), followed by PRM ($15.21 \pm 9.56\%$) and M ($10.9 \pm 0.47\%$). VMM was greater compared to MGM at both stations during PRM and M.

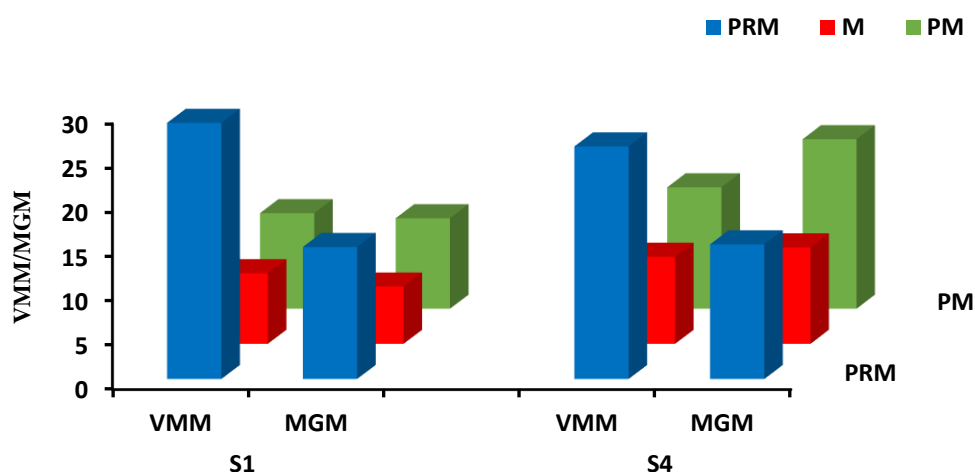


Fig. 5 Seasonal variations in viral mediated mortality (VMM) and microzooplankton grazing mortality (MGM) at S1 and S4 in 2014. pre monsoon (PRM): blue; monsoon (M): red; post monsoon (PM): green

Seasonal variations in viral morphotypes and virally infected prokaryotic morphotypes

TEM analysis of viruses from the study area revealed the dominance of four morphotypes: myoviruses (long contractile tails), siphoviruses (long non-contractile tails), podoviruses (short non-contractile tails) and non-tailed viruses (Fig. 6). Myoviruses were dominant during PRM and PM seasons (48% and 40% , respectively), whereas, non-tailed viruses were the major group during M (38%) (Fig. 7). Non-tailed viruses were the second major group after myoviruses forming 22% , 38% and 28% during PRM, M and PM seasons, respectively. Siphoviruses and podoviruses represented the next most abundant morphotypes.

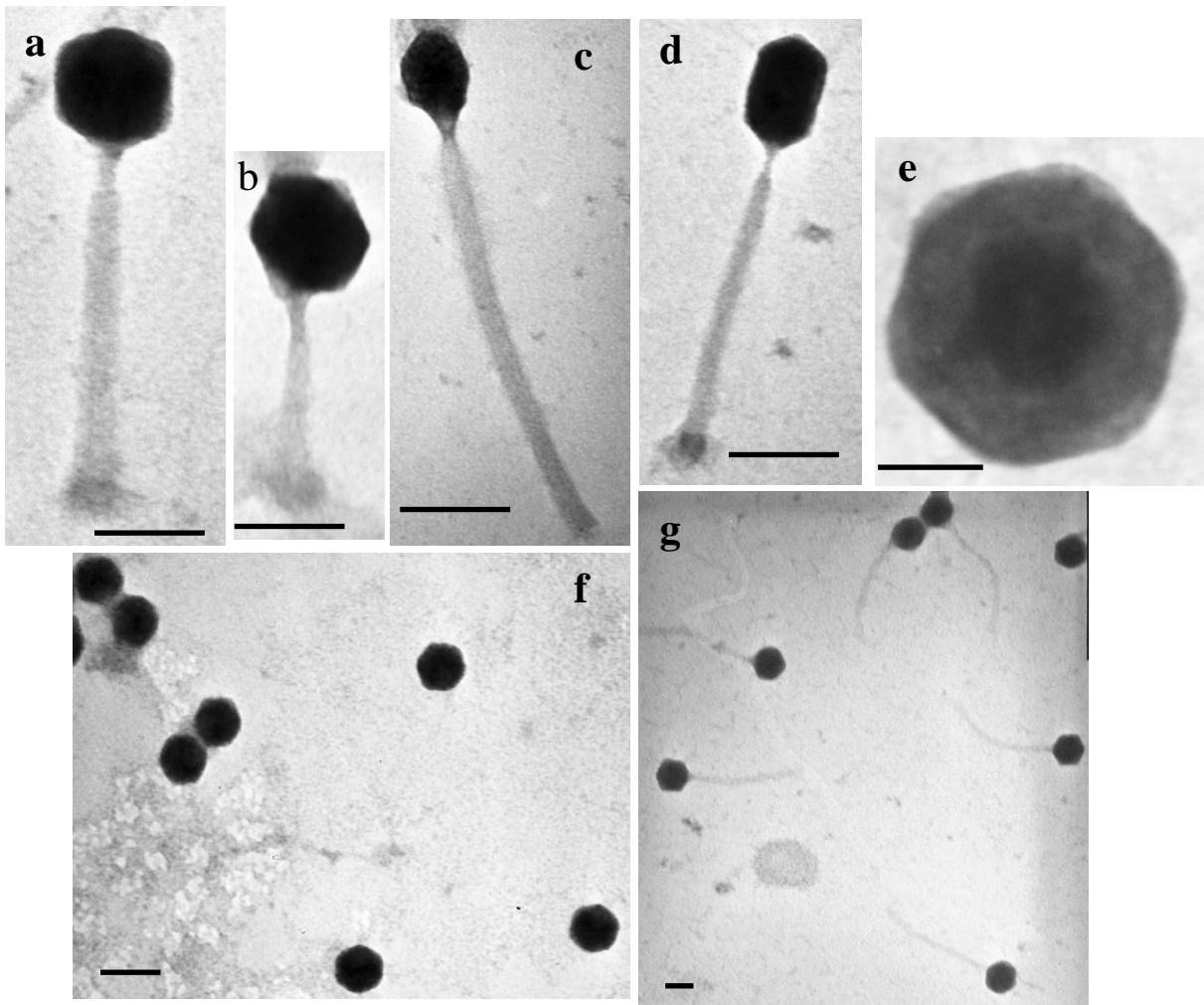


Fig. 6 Viral morphotypes from the Arabian Sea (a, b, c, d) myoviruses, (e, f) non-tailed viruses and (g) siphoviruses. Scale bar = 50 nm

The prokaryotic morphotypes as revealed by TEM analysis belonged to five groups, short rods, elongated rods, fat rods, cocci and filamentous rods (Fig. 8). Overall, the rods represented the major fraction of virally infected cells in the study region. Among rods, elongated rods were the most infected ones during PRM (32%), followed by short rods and fat rods (each representing 22%) (Fig. 7). During M and PM, short rods were the major targets of viruses, representing 32% and 31%, respectively. Cocci were the next target group after rods being 15%, 25% and 17% of the infected cells during PRM, M and PM, respectively. Filamentous forms represented the smallest fraction of virally infected cells consistently in all the seasons (9%, 2% and 5% during PRM, M and PM, respectively).

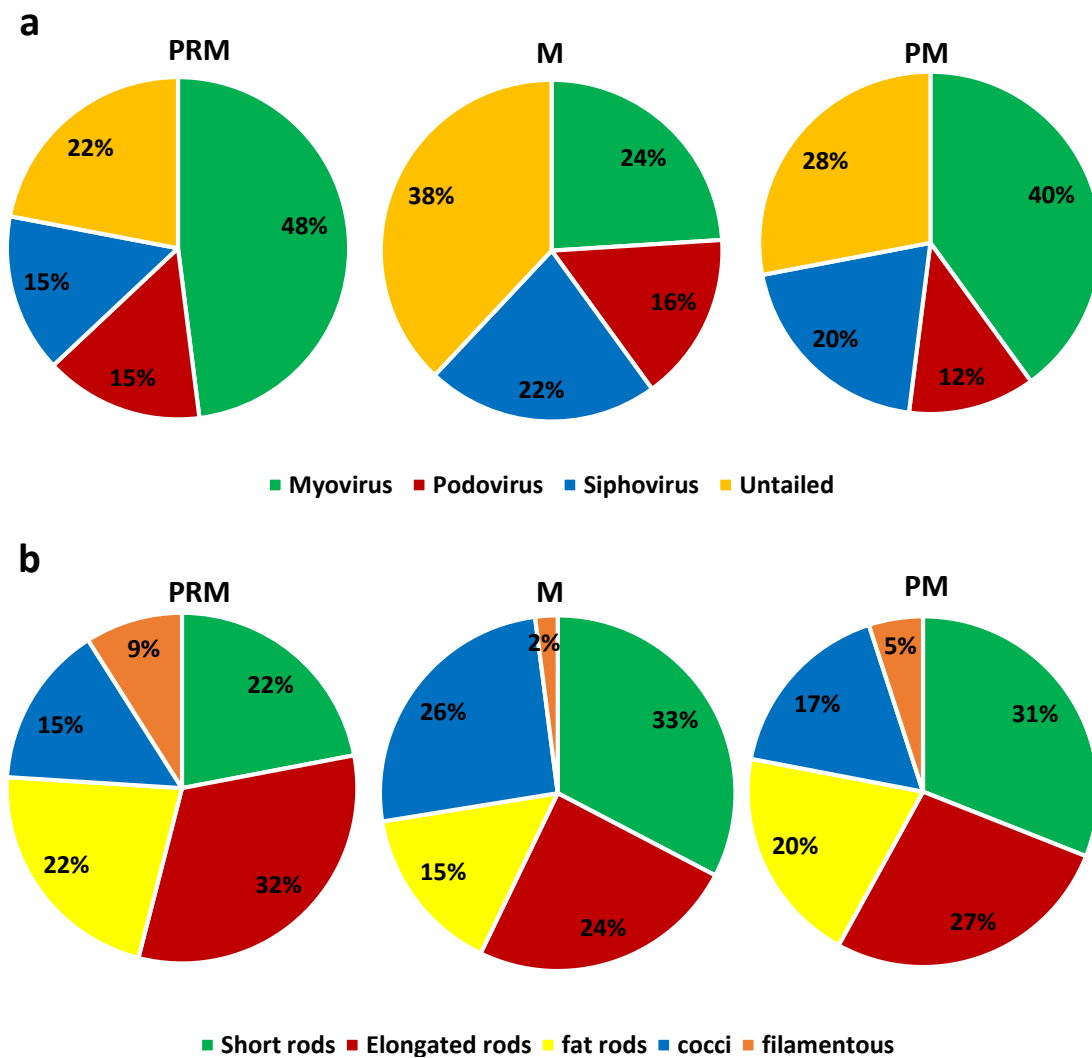


Fig. 7 Seasonal variations in (a) viral morphotypes and (b) infected prokaryotic morphotypes in the study region. PRM: pre-monsoon; M: monsoon; PM: post-monsoon

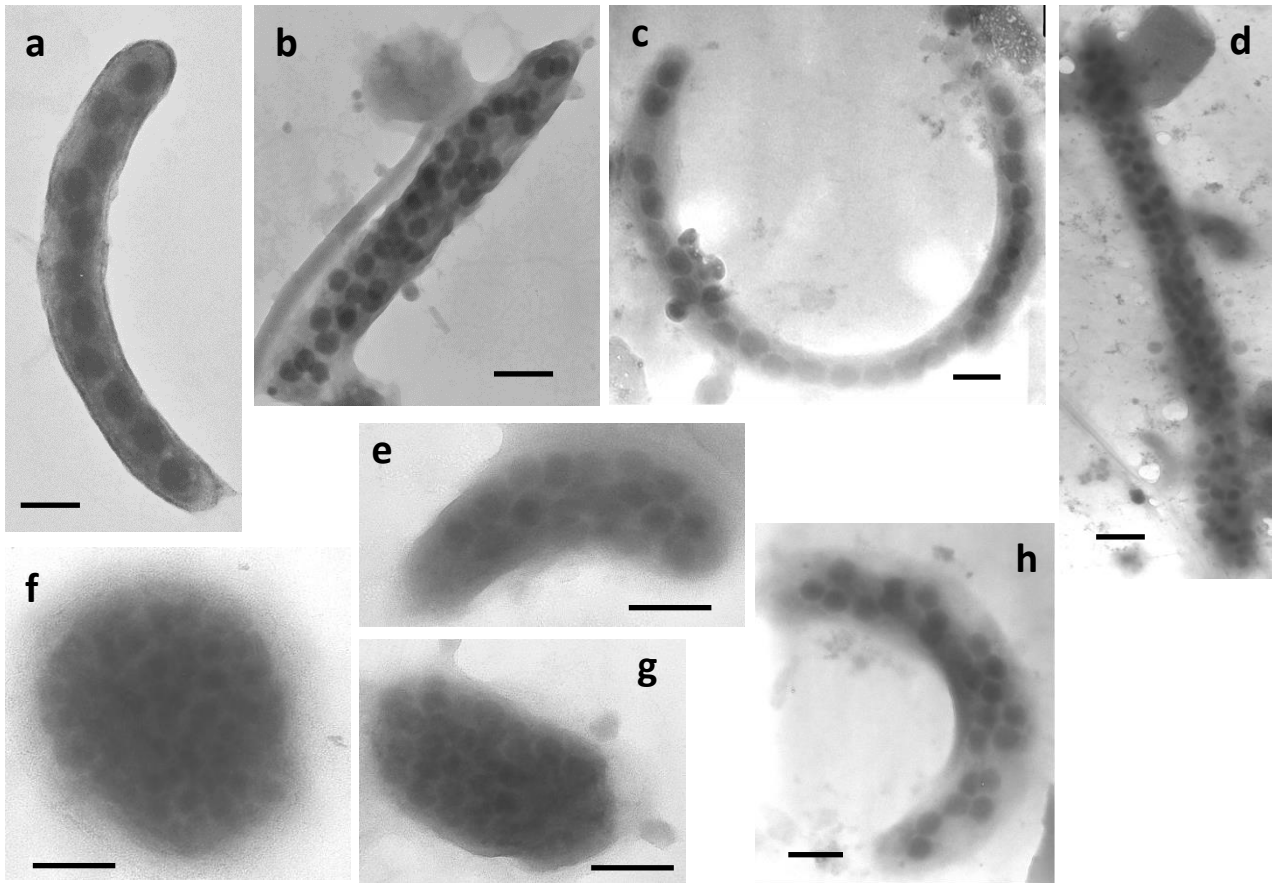


Fig. 8 Viral infected prokaryotic morphotypes in the collected water sample. (a, b, h) long rods, (c, d) filamentous, (f) coccus, (e) short rod and (g) fat rod. Scale bar = 100 nm

Viral burst sizes varied among different prokaryotic morphotypes with filamentous forms having the highest average burst size (81), followed by elongated rods (42), fat rods (36), cocci (30) and short rods (25) (Online Resource 2). Burst sizes of filamentous cells varied greatly with values ranging from 39-122. During PRM, the major fraction of virally infected prokaryotic morphotypes were elongated rods. Percentage of infected filamentous cells were also highest during PRM when compared to the other two seasons (9%, BS: 81). The PCA analysis performed for the two years presents an overview of the seasonal and spatial distribution patterns of VA and PA in relation to other environmental parameters. A clear distinction between the seasonal patterns of different biotic and abiotic variables are obvious in the PCA biplot (Fig. 9). PCA clearly demonstrates that the host abundance (Prokaryotic abundance and Chl *a*) is the major factor influencing the viral abundance and distribution, followed by temperature, salinity and dissolved oxygen. The PC1 axis effectively separated the sampling stations according to the seasonal variation. Factor 1 (PC1) explained 42.63% of the total data variability and was positively correlated with salinity, Chl *a* and inorganic nutrients, but negatively correlated with

temperature and dissolved oxygen. Factor 2 (PC2) explained 32.83% of total data variability and was positively correlated with DO and chlorophyll a in 2014. In 2015, Factor 1 (PC1) explained 60.82% of the total data variability and Factor 2 (PC2) explained 18.30% of total data variability. The nature of correlation parameters with physico-chemical parameters in 2015 were similar to 2014. The inter-relationship of various physico-chemical and biological variables during PRM, M and PM was visualized in distance based redundancy analysis (dbRDA) biplots (Fig 10), highlighting the strong correlations between VA and PA, and the weak correlations with PO₄, SiO₄ and NH₄ in both 2014 and 2015

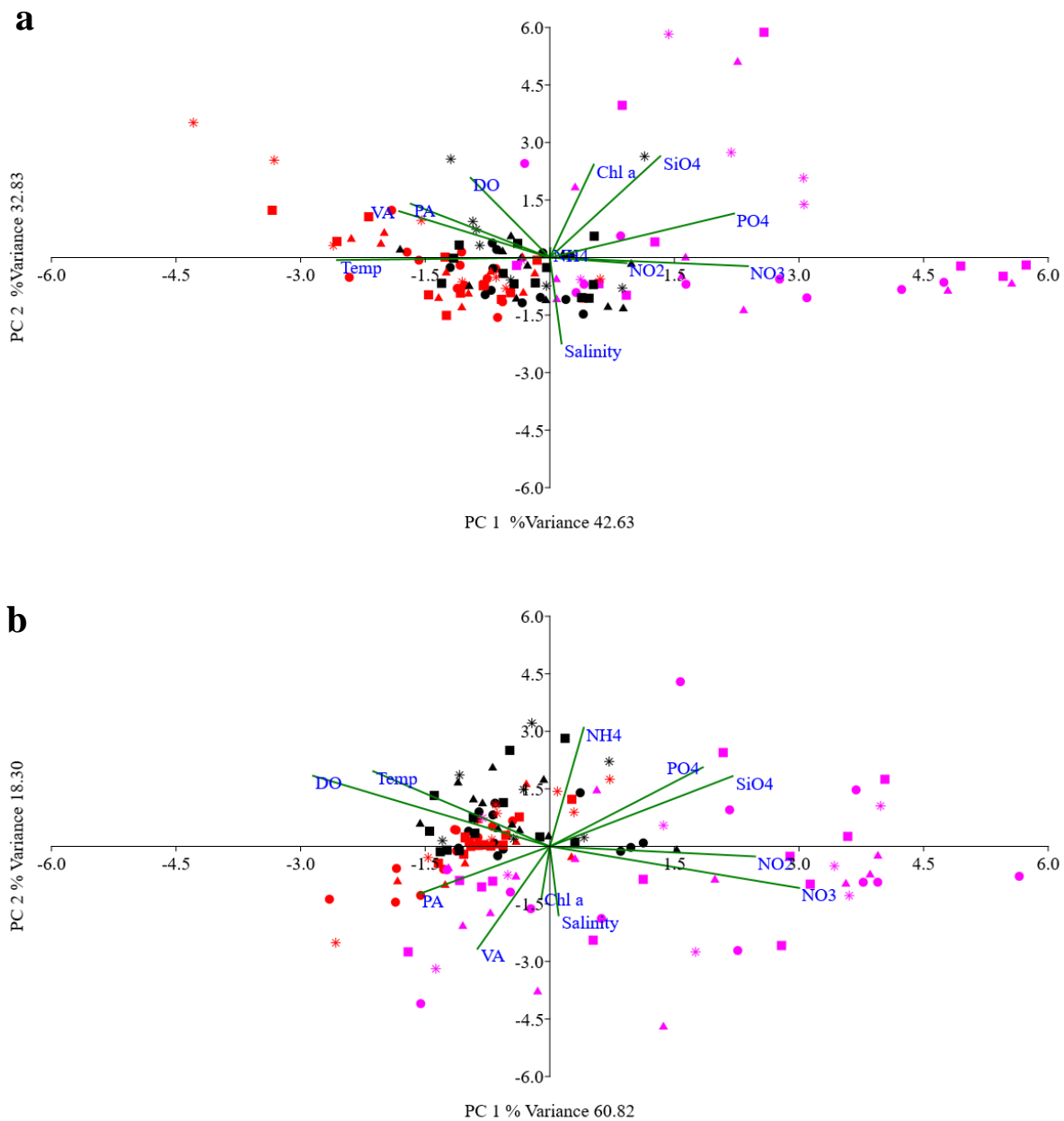
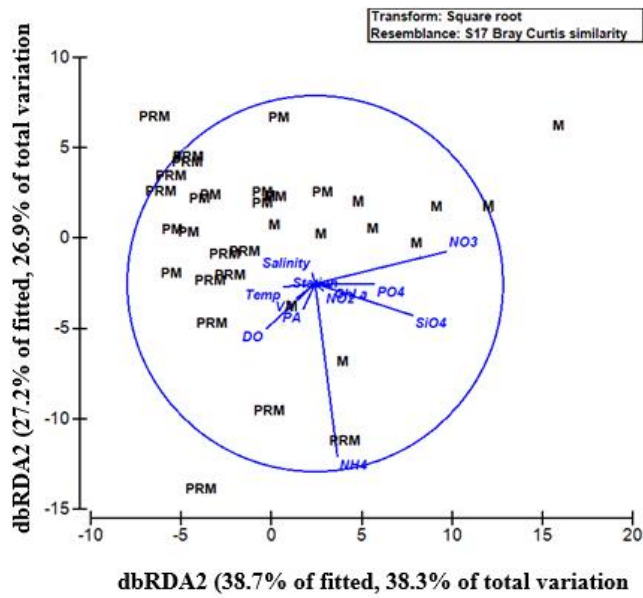


Fig. 9 Principal component analysis (PCA) representing the inter-relationship between various biological and physico-chemical parameters during (a) 2014 and (b) 2015. Observations during pre- monsoon (PRM, red), monsoon (M, pink) and post monsoon (PM, black) from stations, S1 (round), S2 (triangle), S3 (square) and S4 (star). Abbreviations: viral abundance (VA), prokaryotic abundance (PA), chlorophyll *a* (Chl *a*), temperature (Temp), dissolved oxygen (DO), nitrate (NO₃), nitrite (NO₂), ammonium (NH₄), phosphate (PO₄) and silicate (SiO₄)

a



b

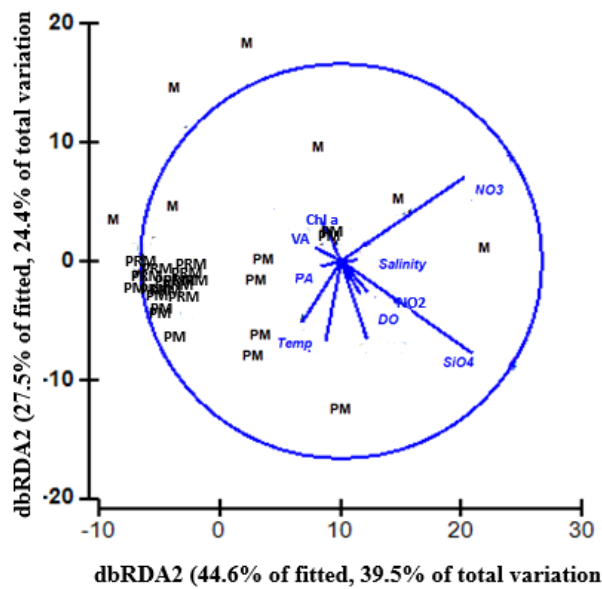


Fig. 10 Distance (dbRDA) showing the inter-relationship of various physico-chemical and biological variables during pre monsoon (PRM), monsoon (M) and post monsoon (PM) in (a) 2014 and (b) 2015. Abbreviations: viral abundance (VA), prokaryotic abundance (PA), chlorophyll *a* (Chl *a*), dissolved oxygen (DO), nitrate (NO₃), nitrite (NO₂), ammonium (NH₄), phosphate (PO₄) and silicate (SiO₄)

Discussion

The present study represents the first description of the influence of seasonality on viral mediated processes in the eastern Arabian Sea (India). The data sets acquired from two consecutive years confirm the existence of a seasonal pattern for most of the studied environmental (biotic and abiotic) variables. A clear seasonality in terms of hydrography prevailed in the studied region. The water column was characterized by high temperature and salinity (Online Resource 3) but with low DO and nutrient concentrations during PRM. During monsoon period (June-Sep), coastal upwelling which brings nutrient rich waters towards the coast. In addition, there are strong cyclonic eddies in the sub-surface waters over the SE Arabian Sea during monsoon (Rao et al., 2008). In the present study, prominent upwelling features like surfacing of cool, less-oxygenated subsurface water mass towards the coast was evident during monsoon. The estuarine and freshwater influx was more in the coastal stations (S3 and S4), which plays a significant role in the distribution of plankton and prokaryotic community. The southwest monsoon period (M) was hence characterized by high nutrient concentrations of NO_3 , PO_4 and SiO_4 . The N:P ratios were comparatively high during M than PRM and PM. Nutrient enrichment favours the growth of phytoplankton and bacteria, which in turn supports the viral proliferation. A recent study by Sabbagh et al. (2020) reported that heterotrophic bacterial abundance is controlled by viruses throughout the year in the Red Sea as evident from the negative correlation between bacterial and viral abundances and positive correlation between bacterial mortality rates and viral abundance. Apart from the indirect effect of nutrient enrichment (such as increased host abundance and metabolism), a number of studies have reported on direct influence of nutrient concentrations, especially, phosphate and nitrate (which positively influence viral nucleic acid and protein syntheses), on viral abundance and viral production (Maat et al. 2014; Motegi et al. 2015).

The abundance of viruses and prokaryotes obtained from this study are comparable to other tropical oceanic regions (Winter et al. 2008; Gainer et al. 2017; Lara et al. 2017). Significant seasonal and spatial variations in the abundance of viruses and prokaryotes were explained from their interaction with various biotic and abiotic components of the system. The dbRDA biplot indicated that prokaryotic abundance was the most important predictor of viral abundance similar to reports from diverse oceanic regions (Middelboe 2000; Taylor et al. 2003; Parsons et al. 2012; Parvathi et al. 2015; De Corte et al. 2016). Another important determinant of viral abundance was temperature. An Artificial Neural Network-based model by Winter et al. (2012) has predicted temperature as the major factor determining prokaryotic and viral abundances. Seasonal variations in environmental parameters, especially temperature and salinity, have been reported to affect the dynamics of host community structure (Suh et al. 2015). Temperature have been reported as one of the key factors influencing

variation in viral and prokaryotic distribution and their interactions over broad spatial and temporal scales (Finke et al. 2017). Increasing temperature was shown to increase bacterial respiration and bacterial production with adequate nutrient supply (Sarmiento et al. 2010). The coupling between bacteria and phytoplankton enhanced with an increase in temperature by 2-6°C (Hoppe et al. 2008). The carbon demand by bacteria also increase by $\approx 20\%$ with increase in temperature without any effect on their growth efficiency (Vazquez-Dominguez et al. 2007). Increase in viral abundance could also be due to switching over of viruses from lytic from lysogenic mode under favorable temperatures (Williamson and Paul 2006). A decrease in latent period, increase in burst size and an increase in viral infectivity were observed with increasing temperature in *Micromonas* viral populations (Maat et al. 2017). In our study, temperature may have affected viral proliferation and activities directly or indirectly by controlling their host abundance and metabolism.

Viral-mediated processes such as host mortality and viral production followed the same seasonal pattern as that of VA and PA with highest values in PRM (Online Resource 4). The existence of a strong and robust relationship between viral production and both viral and prokaryote abundance has been reported from many marine regions (Rowe et al. 2008). Several studies have demonstrated that increasing temperature had a positive influence on host growth rate and subsequently resulted in increased viral production rates (Williamson and Paul 2006; Rowe et al. 2012; Demory et al. 2017). Viral induced mortality of prokaryote and phytoplankton hosts in the present study were greatly influenced by viral production and temperature. Viral mediated mortality of phytoplankton communities has been reported to increase at lower latitudes when compared to higher latitudes where grazer mediated mortality predominated. This shift was associated with an increase in temperature and salinity at lower latitudes (Mojica et al. 2016). Viral lysis has been recognized as a significant means of mortality to the phytoplankton *Phaeocystis globosa* in the North Sea. Viral lysis accounted for 5-66% of the total mortality of *P. globosa* during blooms (Baudoux et al. 2006). Viruses were also found to cause significant mortality to specific picophytoplankton groups in various coastal and oligotrophic marine habitats (Baudoux et al. 2007; Baudoux et al. 2008). In the oligotrophic northeastern Atlantic, viral lysis accounted for the release of 21% of the total carbon produced by picophytoplankton. In the present study, viral lysis accounted for 7.98–28.9% of phytoplankton mortality with highest rates during PRM. High viral production and turnover rates during PRM have been backed by the high burst sizes (42) of elongated rods. High burst sizes along with higher host densities might have possibly contributed to the high infection frequencies and the increased host mortality during this season.

In this study, we evaluated viral morphological characteristics (viral morphotype), and virus-host interactions (infection pattern of viruses on different bacterial morphotypes) using a transmission

electron microscopy (TEM) method during three seasons. Myoviridae was the dominant group in both PRM and PM, followed by untailed viruses. However, during monsoon untailed viruses were the most dominant viral morphotype. Myoviridae form the most dominant group in most marine environments as most viruses are phages, the viruses that infect bacteria (Wommack and Colwell 2000). Myoviruses have a broader host range than other phages, and are capable of infecting different species of bacteria. Few studies have also reported high abundance of non-tailed viruses (Auguet et al. 2006; Stopar et al. 2003; Bratbak et al. 1990). Various environmental parameters such as temperature influences the viral morphological characteristics of myoviridae, and temperature and salinity for untailed viruses and podoviridae (Brum et al. 2013). Several studies suggest that morphological characteristics are linked with seasons and environmental factors are important points to consider when assessing viral persistence (Espinosa et al. 2009). Based on TARA Ocean expedition, myovirus tails were longer in the Arabian Sea than Mediterranean Sea, Red Sea and Atlantic Ocean and capsid diameters of viruses were significantly larger in the Arabian Sea than those in the Indian, Atlantic and Pacific Oceans (Brum et al. 2013). The current study indicates that among different bacterial morphotypes (short rods, elongated rods, fat rods and cocci) rods were the most dominant forms representing about ~75% of the entire bacterial community throughout the study period and were more susceptible to viral infection. When compared to other morphotypes, the elongated rods had highest burst size (42 viruses bacterium⁻¹) probably due to the larger surface area of rods compared to other morphotypes. The present study should guide future work towards understanding the functional roles of the viruses in the southeastern Arabian Sea.

Conclusion

A clear seasonality in viral abundance and various viral processes in the southeastern Arabian Sea is apparent from the present study. Our observations on the seasonal drivers of viral dynamics were similar to those predicted for other oceanic regions such as the North Pacific and the Arctic Ocean. The seasonal variations in host abundance and temperature were the major driving factors of viral processes in the study region. Viral lysis is a significant means of host mortality in the coastal waters of the Arabian Sea especially during premonsoon season. By causing significant percentage of host mortality, viruses may greatly contribute to the dissolved organic matter (DOM) pool. The elevated viral activities during PRM indicated the highly active microbial loop in the oligotrophic premonsoon season. Viral activities along with temperature play crucial role in controlling the host abundance and shaping the host community structure in the Arabian Sea.

Acknowledgement

The authors are thankful to the Director, CSIR-NIO, Goa, India and the Scientist-in-Charge, NIO (RC), Cochin, India for their support and advice. The authors are grateful to Dr. Jyothibabu R. for helping with sample collection.

Funding

This work was supported by Indian National Centre for Ocean Information Services through grant-in-aid project [NIO GAP 2807]. AS is grateful to University Grants Commission (UGC), New Delhi, India for her senior research fellowship grant. JV is grateful to Council of Scientific and Industrial Research (CSIR), New Delhi, for her senior research fellowship grant.

Availability of data and material

The datasets generated during and/or analysed during the current study are available from the corresponding author on reasonable request.

Compliance with ethical standards

Conflict of interest

The authors declare that they have no conflict of interest.

Ethics approval

Not applicable

Consent to participate

All authors give their consent to participate in this publication.

Consent for publication

All authors agree with the content and give consent to publish this manuscript.

Code availability

Not applicable

References

- Auguet JC, Montanie H, Lebaron P (2006) Structure of virioplankton in the Charente Estuary (France): transmission electron microscopy versus pulsed field gel electrophoresis. *Microb ecol* 51:197-208
- Baudoux AC, Noordeloos AA, Veldhuis MJ, Brussaard CP (2006) Virally induced mortality of *Phaeocystis globosa* during two spring blooms in temperate coastal waters. *Aquat Microb Ecol* 44:207-217
- Baudoux AC, Veldhuis MJ, Witte HJ, Brussaard CP (2007) Viruses as mortality agents of picophytoplankton in the deep chlorophyll maximum layer during IRONAGES III. *Limnol Oceanogr* 52:2519-29
- Baudoux AC, Veldhuis MJ, Noordeloos AA, Van Noort G, Brussaard CP (2008) Estimates of virus- vs. grazing induced mortality of picophytoplankton in the North Sea during summer. *Aquat Microb Ecol* 52:69-82
- Binder B (1999) Reconsidering the relationship between virally induced bacterial mortality and frequency of infected cells. *Aquat Microb Ecol* 18:207-215
- Borrel G, Colombe J, Robin A, Lehours AC, Prangishvili D, Sime-Ngando T (2012) Unexpected and novel putative viruses in the sediments of a deep-dark permanently anoxic freshwater habitat. *ISME J* 6:2119
- Bratbak G, Heldal M, Norland S, Thingstad TF (1990) Viruses as partners in spring bloom microbial trophodynamics. *Appl Environ Microbiol* 56:1400-1405
- Breitbart M, Bonnain C, Malki K, Sawaya NA (2018) Phage puppet masters of the marine microbial realm. *Nat Microbiol* 3:754
- Brum JR, Schenck RO, Sullivan MB (2013) Global morphological analysis of marine viruses shows minimal regional variation and dominance of non-tailed viruses. *The ISME J* 7:1738-1751
- Burkill PH, Mantoura RF, Owens NJ (1993) Biogeochemical cycling in the northwestern Indian Ocean: a brief overview. *Deep Sea Res Part II Top Stud Oceanogr* 40:643-649
- Calleja ML, Al-Otaibi N, Morán XA (2019) Dissolved organic carbon contribution to oxygen respiration in the central Red Sea. *Sci Rep* 9: <https://doi.org/10.1038/s41598-019-40753-w>
- Campbell L, Landry MR, Constantinou J, Nolla HA, Brown SL, Liu H, Caron DA (1998) Response of microbial community structure to environmental forcing in the Arabian Sea. *Deep Sea Res Part II Top Stud Oceanogr* 45:2301-2325
- Clokie MR, Millard AD, Mehta JY, Mann NH (2006) Virus isolation studies suggest short-term variations in abundance in natural cyanophage populations of the Indian Ocean. *J Mar Biolog Assoc UK* 86:499-505
- Cram JA, Parada AE, Fuhrman JA (2016) Dilution reveals how viral lysis and grazing shape microbial communities. *Limnol Oceanogr* 61:889-905
- De Corte D, Sintès E, Yokokawa T, Lekunberri I, Herndl GJ (2016) Large-scale distribution of microbial and viral populations in the South Atlantic Ocean. *Environ Microbiol Rep* 8:305-315

- Demory D, Arsenieff L, Simon N, Six C, Rigaut-Jalabert F, Marie D et al (2017). Temperature is a key factor in *Micromonas*-virus interactions. *ISME J* 11:601
- Ducklow HW (1993) Bacterioplankton distributions and production in the northwestern Indian Ocean and Gulf of Oman, September 1986. *Deep Sea Res Part II Top Stud Oceanogr* 40:753-771
- Evans C, Archer SD, Jacquet S, Wilson WH (2003) Direct estimates of the contribution of viral lysis and microzooplankton grazing to the decline of a *Micromonas* spp. population. *Aquat Microb Ecol* 30:207-219
- Finke J, Hunt B, Winter C, Carmack E, Suttle C (2017) Nutrients and other environmental factors influence virus abundances across oxic and hypoxic marine environments. *Viruses* 9:152
- Gainer PJ, Pound HL, Larkin AA, LeClerc GR, DeBruyn JM, Zinser ER, Johnson ZI, Wilhelm SW (2017) Contrasting seasonal drivers of virus abundance and production in the North Pacific Ocean. *PloS One* 12:e0184371
- Gerson VJ, Madhu NV, Jyothibabu R, Balachandran KK, Nair M, Revichandran C (2014) Oscillating environmental responses of the eastern Arabian Sea. *Indian J Mar Sci* 43:67-75
- Grasshoff K, Ehrhardt MKK (1983) *Methods of Seawater Analysis*. Verlag Chemie, Weinheim, Germany
- Hammer O, Harper DA, Ryan PD (2001) PAST: paleontological statistics software package for education and data analysis. *Palaeontol Electron* 4:9
- Hoppe HG, Breithaupt P, Walther K, Koppe R, Bleck S, Sommer U, Jürgens K (2008) Climate warming in winter affects the coupling between phytoplankton and bacteria during the spring bloom: a mesocosm study. *Aquat Microb Ecol* 51:105-115
- Jain A, Bandekar M, Gomes J, Shenoy D, Meena RM, Naik H, Khandeparkar R, Ramaiah N (2014) Temporally invariable bacterial community structure in the Arabian Sea oxygen minimum zone. *Aquat Microb Ecol* 73:51-67
- Jasna V, Parvathi A, Ram ASP, Balachandran KK, Madhu NV, Nair M, Jyothibabu R, Jayalakshmi KV, Revichandran C, Sime-Ngando T (2017) Viral-induced mortality of prokaryotes in a tropical monsoonal estuary. *Front Microbiol* 8:895
- Jasna V, Parvathi A, Aswathy VK, Aparna S, Dayana M, Aswathy AJ, Madhu NV (2019) Factors determining variations in viral abundance and viral production in a tropical estuary influenced by monsoonal cycles. *Reg Stud Mar Sci* 1; <https://doi.org/10.1016/j.rsma.2019.100589>
- Kumar SP, Prasad TG (1996) Winter cooling in the northern Arabian Sea. *Curr Sci* 71:834-841
- Kumar SP, Madhupratap M, Kumar MD, Gauns M, Muraleedharan PM, Sarma VV, De Souza SN (2000) Physical control of primary productivity on a seasonal scale in central and eastern Arabian Sea. *J Earth Syst Sci* 109:433-441
- Lara E, Vaqué D, Sà EL, Boras JA, Gomes A, Borrull E et al (2017) Unveiling the role and life strategies of viruses from the surface to the dark ocean. *Sci Adv* 3:e1602565

- Maat DS, Crawford KJ, Timmermans KR, Brussaard CP (2014) Elevated CO₂ and phosphate limitation favor *Micromonas pusilla* through stimulated growth and reduced viral impact. *Appl Environ Microbiol* 80:3119-3127
- Maat D, Biggs T, Evans C, van Bleijswijk J, van der Wel N, Dutilh B, Brussaard C (2017) Characterization and temperature dependence of Arctic *Micromonas polaris* viruses. *Viruses* 9:134
- Mantoura RFC, Law CS, Owens NJP, Burkhill PH, Woodward EMS, Howland RJM, Llewellyn CA (1993) Nitrogen biogeochemical cycling in the northwestern Indian Deep Sea Res Part II Top Stud *Oceanogr* 40:651-671
- McArdle BH, Anderson MJ (2001) Fitting multivariate models to community data: a comment on distance-based redundancy analysis. *Ecology* 82:290-297
- Middelboe M (2000) Bacterial growth rate and marine virus–host dynamics. *Microb Ecol* 40:114-124
- Mojica KD, Brussaard CP (2014) Factors affecting virus dynamics and microbial host–virus interactions in marine environments. *FEMS Microbiol Ecol* 89:495-515
- Mojica KD, Huisman J, Wilhelm SW, Brussaard CP (2016) Latitudinal variation in virus-induced mortality of phytoplankton across the North Atlantic Ocean. *ISME J* 10:500
- Motegi C, Kaiser K, Benner R, Weinbauer MG (2014) Effect of P-limitation on prokaryotic and viral production in surface waters of the Northwestern Mediterranean Sea. *J Plankton Res* 37:16-20
- Naqvi SWA, Noronha RJ, Somasundar K, Gupta RS (1990) Seasonal changes in the denitrification regime of the Arabian Sea. *Deep Sea Res Part I Oceanogr Res Pap* 37:593-611
- Olson DB, Hitchcock GL, Fine RA, Warren BA (1993) Maintenance of the low-oxygen layer in the central Arabian Sea. *Deep Sea Res Part II Top Stud Oceanogr* 40:673-685
- Ortmann AC, Metzger RC, Liefer JD, Novoveska L (2011) Grazing and viral lysis vary for different components of the microbial community across an estuarine gradient. *Aquat microb ecol* 65:143-157
- Parsons TR, Maita Y, Lalli CM (1984) *A Manual for Biological and Chemical Methods for Seawater Analysis*. Oxford, Pergamon
- Parsons RJ, Breitbart M, Lomas MW, Carlson CA (2012) Ocean time-series reveals recurring seasonal patterns of virioplankton dynamics in the northwestern Sargasso Sea. *ISME J* 6:273
- Parvathi A, Jasna V, Jina S, Jayalakshmy KV, Lallu KR, Madhu NV, Muraleedharan KR, Naveen Kumar KR, Balachandran KK (2015) Effects of hydrography on the distribution of bacteria and virus in Cochin estuary, India. *Ecol Res* 30:85-92
- Parvathi A, Jasna V, Aparna S, Ram ASP, Aswathy V, Balachandran KK, Muraleedharan KR, Mathew D, Sime-Ngando T (2018) High Incidence of Lysogeny in the Oxygen Minimum Zones of the Arabian Sea (Southwest Coast of India). *Viruses* 10:588
- Patel A, Noble RT, Steele JA, Schwalbach MS, Hewson I, Fuhrman JA (2007) Virus and prokaryote enumeration from planktonic aquatic environments by epifluorescence microscopy with SYBR Green I. *Nat Protoc*, 2:269

- Pradeep Ram AS, Arnous B, Danger M, Carrias JF, Lacroix G, Sime-Ngando T (2010) High and differential viral infection rates within bacterial ‘morphopopulations’ in a shallow sand pit lake (Lac de Créteil, France). *FEMS Microbiol Ecol* 74:83-92
- Ramaiah N, Raghukumar S, Gauns M (1996) Bacterial abundance and production in the central and eastern Arabian Sea. *Curr Sci* 71:878-882
- Ramaiah N, Fernandes V, Rodrigues VV, Paul JT, Gauns M (2009) Bacterioplankton abundance and production in Indian Ocean Regions. *Indian Ocean biogeochemical processes and ecological variability* 1:119-132
- Rao AD, Joshi M, Ravichandran M (2008) Oceanic upwelling and downwelling processes in waters off the west coast of India. *Ocean Dyn* 58:213-226
- Rodriguez F, Fernandez E, Head RN, Harbour DS, Bratbak G, Heldal M, Harris RP (2000) Temporal variability of viruses, bacteria, phytoplankton and zooplankton in the western English Channel off Plymouth. *J Mar Biolog Assoc UK* 80:575-586
- Rowe JM, Saxton MA, Cottrell MT, DeBruyn JM, Berg GM, Kirchman DL, Hutchins DA, Wilhelm SW (2008) Constraints on viral production in the Sargasso Sea and North Atlantic. *Aquat Microb Ecol* 52:233-244
- Rowe JM, DeBruyn JM, Poorvin L, LeClerc GR, Johnson ZI, Zinser ER, Wilhelm SW (2012) Viral and bacterial abundance and production in the Western Pacific Ocean and the relation to other oceanic realms. *FEMS Microbiol Ecol* 79:359-370
- Sabbagh EI, Huete-Stauffer TM, Calleja ML, Silva L, Viegas M, Morán XA (2020) Weekly variations of viruses and heterotrophic nanoflagellates and their potential impact on bacterioplankton in shallow waters of the central Red Sea. *FEMS microbiol ecol* 96: <https://doi.org/10.1093/femsec/fiaa033>
- Sarmiento H, Montoya JM, Vázquez-Domínguez E, Vaqué D, Gasol JM (2010) Warming effects on marine microbial food web processes: how far can we go when it comes to predictions? *Philos Trans R Soc Lond B, Biol Sci* 365:2137-2149
- Shelford EJ, Middelboe M, Møller EF, Suttle CA (2012) Virus-driven nitrogen cycling enhances phytoplankton growth. *Aquat Microb Ecol* 66:41-46
- Stopar D, Černe A, Žigman M, Poljšak-Prijatelj M, Turk V (2003) Viral abundance and a high proportion of lysogens suggest that viruses are important members of the microbial community in the Gulf of Trieste. *Microb ecol* 46:249-256
- Suh SS, Park M, Hwang J, Kil EJ, Jung SW, Lee S, Lee TK (2015) Seasonal dynamics of marine microbial community in the South Sea of Korea. *PLoS One* 10:e0131633
- Taylor GT, Hein C, Iabichella M (2003) Temporal variations in viral distributions in the anoxic Cariaco Basin. *Aquat Microb Ecol* 30:103-116
- Thomas R, Berdjeb L, Sime-Ngando T, Jacquet S (2011) Viral abundance, production, decay rates and life strategies (lysogeny versus lysis) in Lake Bourget (France). *Environ Microbiol* 13:616-630

- Vazquez-Dominiguez E, Vaque D, Gasol JM (2007) Ocean warming enhances respiration and carbon demand of coastal microbial plankton. *Glob Chang Biol* 13:1327-1334
- Weinbauer MG, Winter C, Höfle MG (2002) Reconsidering transmission electron microscopy based estimates of viral infection of bacterio-plankton using conversion factors derived from natural communities. *Aquat Microb Ecol* 27:103-110
- Weinbauer MG, Bonilla-Findji O, Chan AM, Dolan JR, Short SM, Šimek K, Wilhelm SW, Suttle CA (2011) Synechococcus growth in the ocean may depend on the lysis of heterotrophic bacteria. *J Plankton Res* 33:1465-1476
- Wiebinga CJ, Veldhuis MJ, De Baar HJ (1997) Abundance and productivity of bacterioplankton in relation to seasonal upwelling in the northwest Indian Ocean. *Deep Sea Res Part I Oceanogr Res Pap* 44:451-476
- Wilhelm SW, Brigden SM, Suttle CA (2002) A dilution technique for the direct measurement of viral production: a comparison in stratified and tidally mixed coastal waters. *Microb Ecol* 43:168-173
- Williamson SJ, Paul JH (2006) Environmental factors that influence the transition from lysogenic to lytic existence in the ϕ HSIC/Listonella pelagia marine phage–host system. *Microb Ecol* 52:217-225
- Winter C, Moeseneder MM, Herndl GJ, Weinbauer MG (2008) Relationship of geographic distance, depth, temperature, and viruses with prokaryotic communities in the eastern tropical Atlantic Ocean. *Microb Ecol* 56:383-389
- Winter C, Payet JP, Suttle CA (2012) Modeling the Winter–to–Summer Transition of Prokaryotic and Viral Abundance in the Arctic Ocean. *PloS one*. 7:e52794
- Wommack KE, Colwell RR (2000) Virioplankton: viruses in aquatic ecosystems. *Microbiol Mol Biol Rev* 64:69-114
- Yang Y, Motegi C, Yokokawa T, Nagata T (2010) Large-scale distribution patterns of virioplankton in the upper ocean. *Aquat Microb Ecol* 60:233-246

Table 1 F values based on three way ANOVA performed for various biotic and abiotic variables in the four stations (S1, S2, S3 and S4) during the three seasons (PRM, M and PM) of 2014 and 2015

	Variables	Year	Season	Station	Year × Season	Year × Station	Season × Station	Year × Season × Station
d		1	2	10	2	10	20	20
f								
	VA	25.246**	8.667**	2.020*	5.544**	0.615	0.442	0.346
	PA	0.169	18.406**	3.154**	0.206	0.712	0.765	0.755
	DO	18.192**	27.056**	5.826**	7.433**	0.788	2.009**	0.760
	NO ₂	0.945	0.888	0.899	0.903	0.898	0.918	0.917
	NO ₃	1.038	60.656**	3.274**	0.407	0.777	3.301**	0.655
	NH ₄	14.098**	1.300	1.315	2.168	1.312	0.869	0.658
	SiO ₄	11.173**	19.990**	2.673**	1.937	0.279	0.563	0.336
	PO ₄	69.661**	34.948**	1.851	33.605**	0.204	0.374	0.246
	Chl <i>a</i>	1.043	11.902**	2.414**	0.282	0.778	2.004	0.726

VA: viral abundance, PA: prokaryotic abundance, Chl *a*: chlorophyll *a*, DO: dissolved oxygen, NO₃: nitrate, NO₂: nitrite, NH₄: ammonium, PO₄: phosphate and SiO₄: silicate. Significant F values at p<0.05 and p<0.001 are represented with * and **, respectively

Table 2 Seasonal and vertical variations in physico-chemical and biological parameters at the four stations (S1-S4) in 2014

Season	Parameters	S1			S2			S3			S4	
		0.5	15	30	0.5	11	22	0.5	7	14	0.5	6
PR M	Depth (m)	0.70	0.41±	0.53±	0.71±	0.50±0.	0.42±	0.75±	0.44±	0.45±	1.17±0.	0.72±0
	VLP/mL)	±0.1	0.00	0.19	0.12	13	0.15	0.38	0.15	0.09	71	.57
	PA (10 ⁶ cells/mL)	0.91	0.53±	0.78±	1.00±	0.86±0.	0.55±	1.06±	0.93±	1.02±	1.55±1.	1.03±0
		±0.4	0.18	0.46	0.57	60	0.24	0.74	0.90	0.74	25	.86
	Chl a	0.36	0.37±	0.51±	0.79±	0.44±0.	1.10±	0.62±	0.52±	0.68±	2.04±2.	1.81±2
		±0.3	0.17	0.16	0.68	41	0.62	0.20	0.31	0.40	15	.18
	DO (mL L ⁻¹)	5.35	6.02±	4.75±	4.65±	4.70±1.	3.85±	5.10±	4.52±	4.82±	4.95±1.	4.27±1
		±1.0	1.15	0.78	1.70	54	1.75	2.15	1.64	2.35	22	.33
	Temperature (°C)	30.55	29.28	29.10	30.40	29.56	29.15	30.39	29.84	29.40	30.60±	29.66±
		±0.5	±0.37	±0.25	±0.76	±0.50	±0.35	±0.84	±1.23	±0.59	0.4	0.66
Salinity (PSU)	34.07	34.32	34.73	34.05	34.2±	34.56	33.83	34.23	33.56	32.67±	33.24±	
	±0.2	±0.15	±0.60	±0.10	0.05	±0.32	±0.25	±0.46	±0.74	2.13	2.49	
Nutrie nts(μ mol L ⁻¹)	NO ₃	0.46	0.36±	0.80±	0.43±	0.64±	1.02±	0.52±	0.66±	0.79±	0.75±0.	1.33±0
		±0.3	0.20	0.77	0.35	0.40	0.52	0.50	0.35	0.61	44	.76
	PO ₄	0.30	0.35±	0.33±	0.59±	0.62±	0.62±	0.50±	0.3±0	0.45±	0.69±0.	0.72±0
		±0.1	0.16	0.38	0.57	0.65	0.70	0.14	.18	0.37	38	.42

M	VA (10⁷ VLP/mL)	0.28	0.21±	0.17±	0.24±	0.23±	0.09±	0.29±	0.22±	0.18±	0.45±0.	0.24±0	
		±0.1	0.05	0.03	0.12	0.09	0.03	0.09	0.13	0.13	13	.11	
		0											
	PA (10⁶ cells/mL)	0.55	0.37±	0.39±	0.39±	0.39±	0.26±	0.53±	0.33±	0.31±	0.57±0.	0.32±0	
		±0.1	0.00	0.19	0.09	0.03	0.15	0.08	0.12	0.09	13	.13	
		2											
	Chl a	1.50	0.76±	0.65±	9.34±	0.98±	1.03±	11.42	0.84±	1.08±	1.86±0.	2.33±1	
		±2.2	0.61	0.75	13.53	0.76	1.11	±16.7	0.85	0.90	91	.24	
		3											
	DO (mL L⁻¹)	6.14	3.68±	2.71±	7.78±	6.23±	2.02±	8.59±	4.06±	1.95±	5.69±1.	7.11±4	
±2.8		1.91	2.87	4.17	1.01	2.24	2.51	3.00	1.49	31	.15		
	6												
Temperature (°C)	27.74	25.89	24.74	27.52	26.71	24.51	27.51	26.72	25.47	27.09±	26.61±		
	±0.3	±1.79	±2.44	±0.71	±1.05	±1.78	±0.56	±1.68	±1.80	0.82	0.98		
	2												
Salinity (PSU)	29.83	34.78	35.16	31.57	34.80	35.22	29.53	33.84	34.56	31.52±	28.16±		
	±7.2	±0.59	±0.32	±3.62	±0.38	±0.33	±6.83	±1.55	±0.87	3.64	11.50		
	3												
Nutrie nts(μ mol L⁻¹)	NO₃	0.89	7.04±	12.91	1.16±	3.95±	14.30	0.81±	8.27±	14.05	2.09±1.	6.45±4	
		±0.2	2.39	±3.73	0.14	1.59	±2.27	0.33	5.26	±11.4	81	.97	
	1												
PO₄	1.27	1.68±	1.90±	1.47±	1.37±	1.93±	1.71±	1.83±	2.27±	2.2±1.6	1.54±1		
	±0.6	0.85	0.84	1.29	0.74	1.27	1.53	1.52	1.63	6	.00		
	9												
PM	VA (10⁷ VLP/mL)	0.31	0.19±	0.20±	0.40±	0.22±	0.12±	0.35±	0.31±	0.19±	0.50±0.	0.26±0	
		±0.1	0.11	0.17	0.26	0.19	0.05	0.22	0.18	0.08	11	.09	
		5											
	PA (10⁶ cells/mL)	0.57	0.41±	0.36±	0.66±	0.37±	0.30±	0.55±	0.43±	0.41±	0.87±0.	0.45±0	
±0.1		0.17	0.08	0.45	0.13	0.09	0.23	0.13	0.17	33	.08		
	7												
Chl a	0.27	0.32±	0.43±	0.58±	0.37±	0.58±	0.59±	0.65±	0.60±	1.33±1.	1.08±0		
	±0.2	0.25	0.26	0.36	0.29	0.33	0.46	0.49	0.34	01	.71		
	8												

DO (mL L⁻¹)	7.44 ±1.4 4	6.59± 2.11	5.26± 2.01	6.77± 1.26	5.76± 2.43	4.97± 1.75	6.75± 1.10	5.76± 1.3	5.38± 1.39	7.72±3. 27	5.73±1 .53	
Temperature (°C)	29.06 ±0.4 4	28.81 ±0.31	28.27 ±0.41	29.27 ±0.45	28.71 ±0.39	28.57 ±0.26	29.53 ±0.61	28.9± 0.31	28.61 ±0.31	29.57± 0.89	28.90± 0.88	
Salinity (PSU)	32.98 ±1.3 5	34.54 ±0.88	35.08 ±0.72	31.60 ±2.14	34.29 ±1.12	34.86 ±0.63	30.88 ±3.76	33.98 ±0.52	34.57 ±0.71	29.48± 2.06	34.23± 1.62	
Nutrients (μmol L⁻¹)	NO₃	1.45 ±1.2 3	1.00± 0.46	1.07± 0.55	1.00± 1.12	1.73± 1.30	1.43± 0.60	1.79± 1.86	1.43± 1.11	1.14± 0.61	2.40±1. 18	1.50±1 .00
	PO₄	0.39 ±0.2 9	0.32± 0.13	0.42± 0.13	0.46± 0.19	0.50± 0.33	0.54± 0.26	0.58± 0.50	0.44± 0.45	0.83± 0.19	0.91±0. 76	0.67±0 .39

PRM: pre monsoon, M: monsoon, PM: post monsoon, VA: viral abundance, PA: prokaryotic abundance, DO: dissolved oxygen, NO₃: nitrate, PO₄: phosphate

Table 3 Seasonal and vertical variations in physico—chemical and biological parameters at the four stations (S1-S4) in 2015

Season	Parameters	S1			S2			S3			S4		
PR M	Depth (m)	0.5	15	30	0.5	11	22	0.5	7	14	0.5	6	
	VA (10⁷ VLP/mL)	1.47 ±0.6	0.65± 0.39	0.59± 0.90	0.92± 0.42	0.50±0.44	0.54± 0.33	0.89± 0.38	0.76± 0.91	0.65± 0.24	1.12± 1.29	0.70± 0.63	
	PA (10⁶ cells/mL)	2.34 ±1.6	0.63± 0.54	0.97± 1.87	0.39± 0.39	0.48±0.41	0.53± 0.42	0.59± 0.28	0.69± 1.02	0.49± 0.46	1.98± 2.13	0.73± 0.44	
	Chl a	0.2± 0.30	0.10± 0.12	0.53± 0.17	0.27± 0.24	0.32±0.21	0.64± 0.20	0.49± 0.36	0.40± 0.29	0.57± 0.16	1.01± 0.66	1.30± 0.49	
	DO (mL L⁻¹)	7.05 ±0.1	6.92± 0.34	6.77± 0.82	6.98± 0.56	6.69±0.39	6.29± 1.08	6.39± 0.25	6.39± 0.25	6.05± 0.26	6.14± 0.53	5.59± 1.04	
	Temperature (°C)	30.37 ±0.7	29.87 ±0.68	29.4± 0.46	30.49 ±0.62	30.08 ±0.69	29.54 ±0.54	30.47 ±0.39	29.88 ±0.60	29.81 ±0.58	31.10 ±0.82	30.44 ±0.38	
	Salinity (PSU)	34.04 ±0.3	34.19 ±0.33	33.04 ±2.1	33.41 ±1.38	34.22 ±0.23	32.51 ±2.73	32.51 ±1.56	34.02 ±0.18	34.05 ±0.20	32.85 ±0.88	32.96 ±1.42	
	Nutrients (μmol L⁻¹)	NO₃	2.07 ±1.0	1.19± 0.24	1.23± 0.57	1.44± 0.50	1.21± 0.26	2.56± 0.76	2.00± 1.08	1.78± 1.52	1.36± 0.72	1.80± 0.58	2.34± 0.75
		PO₄	0.23 ±0.1	0.36± 0.23	0.28± 0.15	0.20± 0.03	0.33± 0.30	0.32± 0.24	0.50± 0.23	0.41± 0.28	0.37± 0.09	0.79± 0.43	0.79± 0.60
	M	VA (10⁷ VLP/mL)	1.60 ±1.6	0.78± 0.59	0.13± 0.08	0.85± 0.62	1.21± 1.64	1.26± 1.62	0.74± 0.31	0.76± 0.43	0.99± 0.98	1.26± 1.42	0.46± 0.36

	PA (10⁶ cells/mL)	0.78 ±0.9	0.39± 0.46	0.10± 0.16	0.28± 0.38	0.33± 0.30	0.30± 0.18	0.61± 0.66	0.53± 0.37	0.39± 0.29	0.76± 0.77	0.39± 0.43
	Chl a	1.97 ±1.2	1.75± 0.88	0.69± 0.53	2.07± 1.89	2.55± 0.75	2.34± 1.02	1.83± 1.21	4.13± 0.85	2.82± 1.22	2.98± 1.35	2.29± 0.88
	DO (mL L⁻¹)	7.57 ±1.1	3.48± 2.57	1.69± 1.76	7.38± 1.25	4.48± 3.51	3.25± 3.73	6.58± 1.8	5.01± 3.47	3.34± 3.79	6.32± 0.65	2.88± 2.54
	Temperature (°C)	25.70 ±0.5	24.22 ±0.53	23.09 ±0.35	26.2± 0.75	25.42 ±0.83	24.01 ±0.75	26.52 ±1.68	24.86 ±0.93	24.12 ±0.85	26.35 ±1.2	24.22 ±0.56
	Salinity (PSU)	34.73 ±0.4	34.81 ±0.56	34.88 ±1.23	33.94 ±5.81	34.48 ±1.35	34.90 ±4.68	29.18 ±8.60	34.84 ±0.53	30.66 ±0.73	32.78 ±7.3	34.58 ±2.06
	Nutrients(μ mol L⁻¹)											
	NO₃	2.38 ±2.1	7.33± 9.01	17.94 ±3.81	2.41± 2.11	4.93± 3.20	12.06 ±6.86	7.67± 9.12	5.01± 3.31	9.82± 9.97	6.91± 10.41	7.08± 7.09
	PO₄	0.15 ±0.1	0.23± 0.21	0.5±0 .48	0.13± 0.13	0.32± 0.30	0.57± 0.56	0.44± 0.55	0.35± 0.31	0.54± 0.67	0.41± 0.46	0.45± 0.43
	VA (10⁷ VLP/mL)	0.61 ±0.1	0.46± 0.15	0.34± 0.11	0.46± 0.17	0.27± 0.15	0.19± 0.04	0.58± 0.22	0.42± 0.13	0.42± 0.16	0.70± 0.24	0.58± 0.22
	PA (10⁶ cells/mL)	0.28 ±0.2	0.23± 0.14	0.16± 0.17	0.28± 0.31	0.17± 0.16	0.16± 0.16	0.75± 0.20	0.55± 0.23	0.52± 0.12	0.76± 0.10	0.58± 0.06
PM	Chl a	0.33 ±0.4	0.27± 0.36	0.29± 0.08	0.78± 0.98	0.54± 0.07	0.37± 0.16	0.55± 0.45	0.63± 0.02	0.43± 0.24	0.97± 0.07	1.21± 0.96
	DO (mL L⁻¹)	8.06 ±1.2	6.85± 2.19	7.39± 1.37	9.95± 0.73	7.81± 0.97	6.77± 2.56	8.72± 1.43	8.38± 1.39	7.56± 0.60	7.93± 1.36	7.41± 1.00

Temperature (°C)	28.68	28.59	28.16	28.73	28.47	28.42	29.32	28.60	28.41	29.22	28.82	
	±0.6	±0.44	±0.20	±0.58	±0.20	±0.14	±0.83	±0.22	±0.06	±0.18	±0.04	
1												
Salinity (PSU)	32.73	34.80	34.94	32.78	34.59	34.81	30.14	34.17	34.75	29.92	33.86	
	±2.0	±0.83	±1.01	±2.04	±0.39	±0.71	±6.04	±0.25	±0.57	±4.94	±0.14	
5												
Nutrie	NO₃	2.59	1.73±	1.99±	1.71±	0.30±	2.08±	1.58±	0.25±	0.62±	2.63±	1.26±
		±1.7	2.13	2.23	1.67	0.20	3.43	1.92	0.07	0.24	2.48	1.63
2												
1) mol L ⁻¹)	PO₄	0.35	0.20±	0.38±	0.31±	0.30±	0.41±	0.36±	0.33±	0.4±0	0.49±	0.38±
		±0.2	0.14	0.07	0.12	0.25	0.22	0.29	0.,15	.31	0.31	0.30
8												

PRM: pre monsoon, M: monsoon, PM: post monsoon, VA: viral abundance, PA: prokaryotic abundance, DO: dissolved oxygen, NO₃⁻: nitrate and PO₄³⁻: phosphate

Figure Legends

Fig 1 Sampling locations in the Arabian Sea. Water samples were collected from four stations of a transect perpendicular to the coast of Kochi on monthly basis during 2014 and 2015. Sampling locations are marked as S1, S2, S3 and S4

Fig. 2 Variations in viral and prokaryotic abundance (VA & PA) during pre-monsoon (PRM, blue), monsoon (M, red) and post-monsoon (PM, green) seasons. (a) VA in 2014, (b) VA in 2015, (c) PA in 2014 and (d) PA in 2015

Fig. 3 Variations in (a) viral production (VP) and (b) viral turnover rates (VTR) at stations S1 and S4 during pre-monsoon (PRM, blue), monsoon (M, red) and post-monsoon (PM, green) in 2014

Fig. 4 Seasonal variations in (a) frequency of infected cells (FIC) and (b) viral induced prokaryotic mortality (VIPM) at S1 and S4 in 2014. Pre-monsoon (PRM): blue; monsoon (M): red; post-monsoon (PM): green

Fig. 5 Seasonal variations in viral mediated mortality (VMM) and microzooplankton grazing mortality (MGM) at S1 and S4 in 2014. pre-monsoon (PRM): blue; monsoon (M): red; post-monsoon (PM): green

Fig. 6 Viral morphotypes from the Arabian Sea (a, b, c, d) myoviruses, (e, f) non-tailed viruses and (g) siphoviruses. Scale bar = 50 nm

Fig. 7 Seasonal variations in (a) viral morphotypes and (b) infected prokaryotic morphotypes in the study region. PRM: pre-monsoon; M: monsoon; PM: post-monsoon

Fig. 8 Viral infected prokaryotic morphotypes in the collected water sample. (a, b, h) long rods, (c, d) filamentous, (f) coccus, (e) short rod and (g) fat rod. Scale bar = 100 nm

Fig. 9 Principal component analysis (PCA) representing the inter-relationship between various biological, physical and chemical parameters during (a) 2014 and (b) 2015. Observations during pre-monsoon (PRM, red), monsoon (M, pink) and post-monsoon (PM, black) from stations, S1 (round), S2 (triangle), S3 (square) and S4 (star). Abbreviations: viral abundance (VA), prokaryotic abundance (PA), chlorophyll *a* (Chl *a*), temperature (Temp), dissolved oxygen (DO), nitrate (NO₃), nitrite (NO₂), ammonium (NH₄), phosphate (PO₄) and silicate (SiO₄)

Fig. 10 Distance based linear model (DistLM) showing the inter-relationship of various physical, chemical and biological variables during pre-monsoon (PRM), monsoon (M) and post-monsoon (PM) in (a) 2014 and (b) 2015. Abbreviations: viral abundance (VA), prokaryotic abundance (PA), chlorophyll *a* (Chl *a*), dissolved oxygen (DO), nitrate (NO₃), nitrite (NO₂), ammonium (NH₄), phosphate (PO₄) and silicate (SiO₄)

Online Resource 1 Variations in (a & b) temperature, (c & d) salinity and (e & f) Chl *a* at the four stations, S1-S4 during pre-monsoon (PRM, blue), monsoon (M, red) and post-monsoon (PM, green)

Online Resource 2 Variations in the number of average progenies produced per infected cells (burst size) of different prokaryotic morphotypes

Online Resource 3 Vertical profiles of temperature and salinity illustrating the seasonal changes in hydrography. (a-c) PRM (pre monsoon), M (monsoon) & PM (post monsoon) seasons in 2014, (d-f) PRM, M & PM seasons in 2015

Online Resource 4 Principal component analysis (PCA) representing different biological, physical and chemical factors influencing viral processes in the study region during 2014. Premonsoon (PRM, green), monsoon (M, black), and post monsoon (PM, red). Abbreviations: viral abundance (VA), prokaryotic abundance (PA), viral production (VP), viral turnover rate (VTR), frequency of visibly infected cells (FVIC), frequency of infected cells (FIC), viral induced prokaryotic mortality (VIPM), viral mediated mortality of phytoplankton (VMM), microzooplankton grazing mortality (MGM), chlorophyll *a* (Chl *a*), temperature (Temp), dissolved oxygen (DO), nitrate (NO₃), nitrite (NO₂), ammonium (NH₄), phosphate (PO₄) and silicate (SiO₄)